ENDOTHELIAL CHARACTERISTICS OF CARDIAC RESIDENT STEM CELL ANTIGEN-1^{+} AND C-KIT^{+} CELLS

by

Kirishani Kesavan

Submitted in partial fulfillment of the requirements

for the degree of Master of Science

at

Dalhousie University

Halifax, Nova Scotia

July 2022

Table of Contents

List of Figures

Abstract

Background: Stem cell antigen-1 (Sca-1) and c-kit have been extensively used as cell surface markers to identify stem cells in various organs. In the heart, these were originally suggested to be markers for the intrinsic cardiac myocyte stem cells; however, a growing body of evidence now suggests that the majority of Sca-1^+ or c-kit^+ cells in the heart are of endothelial lineage. These cells may play an important role in vascular adaptation during cardiac remodelling and pathophysiological heart diseases. However, endothelial functions of these cells have not been studied. Furthermore, there is no information regarding differences in the abundance of this population across ventricles, sexes, strains of rat, and in right ventricle pathological conditions.

Purpose: The purpose of this thesis was to examine the endothelial cell characteristics of cardiac Sca-1^+ cells and c-kit^+ expressing cells, and assess the distribution across ventricles, sexes, strains, and in a model of RV overload.

Hypothesis: We hypothesize that cardiac resident Sca-1^+ cells and c-kit^+ cells are endothelial precursor/progenitor cells and have angiogenic function. Biological sex, genetic background, and disease state affect abundance of these cells.

Methods: Hearts from adult male and female Sprague Dawley (SD) and Fischer CDF rats were excised and digested to obtain a single-cell suspension. Cells were then stained with stem cell (Sca-1 and c-kit) and endothelial cell (CD31) markers, and analyzed using flow cytometry to determine the abundance of the cell population. Sca-1^+ cells were isolated through magnetic sorting to assess endothelial cell characteristics, such as cell morphology, acetylated low density lipoprotein uptake, lectin binding, and network formation, when cultured on Matrigel. To study the changes during pathological cardiac remodelling, flow cytometry analysis of the Fischer CDF rat hearts was performed at 4 weeks after monocrotaline injection (MCT; 60 mg/kg, sc).

Results: A majority of Sca-1^+ cells and c-kit^+ cells in the heart were $CD31^+$. Sca-1^+ cells isolated from SD rat hearts demonstrated lectin binding and of uptake acetylated low-density lipoprotein. The right ventricle (RV) of the heart had more c-kit^+CD31^+ cells and Sca-1^+CD31^+ cells than the left ventricle (LV). In normal healthy rats, the abundance of c-kit^+CD31^+ cells and Sca- 1^+CD31^+ cells in the RV of male rats were similar to the RV of female rats. MCT treatment led to an increase in RV systolic pressure (RVSP) and RV hypertrophy, which was associated with a marked reduction in abundance of c-kit^+CD31^+ or Sca-1^+CD31^+ cells in the RV.

Conclusions and Clinical Significance: The c-kit or Sca-1 expressing cells in the heart are resident endothelial progenitor-like cells. These cells are highly abundant in the RV, and a marked reduction in abundance of these cells is observed during pathological RV remodelling. Considering the higher abundance of these cells in the RV, these cells may also play a role in vascular adaptation during RV remodeling. It is important to note that RV angiogenesis has been shown to be critical for maintenance of RV function.

List of Abbreviations Used

α-SMA – α smooth muscle actin

AcLDL – acetylated low-density lipoprotein

ANOVA – Analysis of variance

BSA – Bovine serum albumin

CAC – Circulating angiogenic cells

CCAC – Canadian Council on Animal Care

CD31 – Cluster of differentiation 31 (PECAM-1)

CD34 – Cluster of differentiation 34

CD117 – Cluster of differentiation 117 (c-kit)

CD133 – Cluster of differentiation 133

CEPC – Cardiac endothelial progenitor cell

CFU-EC – Colony forming unit endothelial cells

CS-FBS – Charcoal-stripped FBS

cTnT – cardiac troponin T

c-kit – proto-oncogene c-KIT (RTK)

DAPI – 4',6-diamidino-2-phenylindole

EDTA – ethylenediaminetetraacetic acid

EGM2 – Endothelial growth media 2

EGM-2MV – Endothelial growth media 2 microvasculature

eNOS – endothelial nitric oxide synthase

EPC – endothelial progenitor cell

ER-α – Estrogen receptor-α

FI – Fulton Index

FSC – Forward scatter

FSC-A – Forward scatter-area

GPI – glycosyl phosphatidylinositol

GPI-AP – glycosyl phosphatidylinositol-anchored protein

GS – Griffonia simplicifolia

HFpEF – Heart failure with preserved ejection fraction

HFrEF – Heart failure with reduced ejection fraction

HR – Heart rate

IgG – Immunoglobulin G

IL-1α – Interleukin-1 α

IL-1β – Interleukin-1 β

IL-6 – Interleukin-6

kDa – kilodalton

LDL – Low density lipoprotein

LHF – left heart failure

LV – left ventricle

LV+S – Left ventricle + Septum

MAPK – Mitogen-activated protein kinase

MCT – Monocrotaline

MCT-P – Monocrotaline-pyrolle

MI – myocardial infarction

miR-126 – MicroRNA 126

Nkx2.5 – NK2 Homeobox 5, cardiomyocyte marker

PA – Pulmonary artery

PAB – Pulmonary artery banding

PAH – Pulmonary artery hypertension

PBS – Phosphate buffered saline

PBS-T – Phosphate buffered saline-Tris 30

PECAM-1 – platelet endothelial cell adhesion molecule

p-ERK – Phosphorylated extracellular signal-regulated kinases

PI3K – Phosphatidylinositol-3'-kinase

PFA - Paraformaldehyde

PH – Pulmonary hypertension

RAAS – Renin angiotensin aldosterone system

RHF – right heart failure

RTK – receptor tyrosine kinase

RV – right ventricle

RVSP – right ventricular systolic pressure

Sca-1 – Stem cell antigen-1

SD – Sprague Dawley

SCF – Stem cell factor

SSC – Side scatter

SSC-A – Side scatter-area

SSC-H – Side scatter-height

SUHx – Sugen hypoxia

SU5416 – Sugen 5416

TAPSE – Tricuspid annular plane systolic excursion

Tie2 – Angiopoietin-1 receptor, marker of endothelial cells

TNF-α – Tumour necrosis factor α

VEGF – Vascular endothelial growth factor

VEGFR – Vascular endothelial growth factor receptor

Acknowledgements

I am thankful to have had the opportunity to conduct this research project with the help of many people. Firstly, I would like to thank my supervisor, Dr. Ketul Chaudhary, for his expertise, insight, and immense support throughout my degree. His guidance has helped with my personal development as a researcher and student. His time and effort into my mentorship has been constant and endless, and I am forever grateful.

I would also like to thank my supervisory committee, Dr. Xianping Dong, Dr. Yassine El Hiani, Dr. Alex Quinn, and Dr. Keith Brunt, for their guidance with the project. Their advice has provided me with the opportunity to grow as a researcher.

I would like to extend my thanks to my fellow lab members. Sheethal Panchakshari has been instrumental to the development of this project, and I am thankful for her assistance. Erica Seelemann, and Tony El Rabahi have also aided my pursuit through their continuous encouragement and support. I am also thankful to have had the opportunity to work with our undergraduate lab members, who have provided insight to my project, as well.

As the recipient of the Departmental Entrance Scholarship, I would like to thank the Department of Physiology and Biophysics for their continuous support. Furthermore, my appreciation also is for the funding agencies that have supported our project. Dalhousie Medical Research Foundation (DMRF), ResearchNS, the Dalhousie Cardiac Research Excellence Wave (DalCREW), and Dalhousie University have given us the resources needed for a project of our scope. I also offer my thanks to everyone who has supported me throughout my master's degree.

I would also like to thank the Carlton Animal Care Facility, Flow Cytometry CORE, Histology & Research Services Lab, and the Cellular & Molecular Digital Imaging Facility.

A special thank you is reserved for the rats used in the study.

Lastly, I would like to express my deepest love and appreciation for my parents. My parents have given me enough support to last a lifetime, and I am grateful for their warmth, and guidance. My gratitude is extended to my sister, Ajhani Kesavan, for being an academic role model, as well as a supportive friend throughout my degree. Thank you for everything.

CHAPTER 1. INTRODUCTION

1.1 Stem Cells

1.1.1 General Introduction to Stem Cells

Cells are the basic biological functional unit of life. With their ability to proliferate, migrate, send chemical signals, and synthesize various molecules important for biological functions, cells perform a multitude of physiological functions to sustain life. To efficiently perform cellular functions, cells must become specialized through morphological and functional changes. This happens through a complex differentiation pathway, which occurs at a large scale in utero[1]; however, this process continues post birth, and contributes to repair and limited regeneration of various organs[2]. Many tissues contain cells that have not undergone differentiation and are categorized as stem cells[3]. Stem cells are the cells that have the ability to give rise to multiple cell types and have the ability to self-renew (rapidly divide and replenish its number of cells).

The discovery of stem cells is attributed to Ernest McCulloch and James Till in the early 1960's[4]. In this study, the researchers were able to show a linear relationship between the number of transplanted bone marrow cells, with the number of colonies developing in the spleen, in irradiated mice. It was found that these cells had the potential to become three types of specialized cells; red blood cells, white blood cells, and platelets[5]. The researchers also found that the survival curve of colony forming cells that had been irradiated, resembles the survival curve for single cells in culture. With these two findings, they hypothesized that each spleenocyte colony formed, was a clone of a single bone marrow cell. Later, the same group was able to determine that these cells had the ability to self-renew[6]. With the ability to differentiate into specialized cells, and to self-renew, research began to focus on stem cells for their physiological relevance, and therapeutic potential.

Stem cells can be classified based on their differentiation potential. For example, zygote cells have nearly limitless differentiation potential, and are classified as totipotent stem cells[7]. Cells from the inner cell mass of embryos have the ability to form all three germ layers, and are known as pluripotent stem cells[7]. Cells that can give rise to all cell types within a particular lineage (such as mesenchymal stem cells which give rise to bone, muscle, cartilage, and fat) are known as multipotent stem cells[7]. Finally, unipotent cells can only give rise to one type (such as progenitor cells)[7]. Adult stem cells (such as bone marrow cells) typically have more limited differentiation capacity, compared to embryonic stem cells[7].

In 2006, the Yamanaka lab was able to take adult mouse fibroblasts and create induced pluripotent stem cells (iPSCs) through the addition of four factors[8]. These cells demonstrate differentiation capacity similar to embryonic stem cells[8]. With the discovery iPSCs, the possible applications of stem cells in medical research have expanded by many folds[9]. Currently, stem cell research covers vast areas ranging from cell biology, physiology, drug testing, and disease modelling, to organ bioengineering[10]. Therefore, better understanding of stem cells and their physiological relevance can open new avenues for improvement of outcomes of current therapeutic approaches and the development of novel ways to treat incurable diseases[11].

1.1.2 Cell Surface Markers for Stem Cells

To be able to understand stem cell physiology, the need to identify these cells is apparent. The plasma membrane of cells contains various proteins or carbohydrate groups, which are important for various processes, such as cell anchoring, propagating extracellular signals to the inside of the cell, as well as to facilitate cell-to-cell interactions[12]. Many of

these groups are specific to the cell type and investigating the expression of these biomolecules can further elucidate the identity of a cell population[13]. A specific protein, glycoprotein, or a group of proteins that distinguish a cell or subset of cells from another defined subset of cells are termed as a cell surface marker. Two important cell surface markers that are commonly used to identify stem cells in various tissues are stem cell antigen-1 (Sca-1), and c-kit[14].

Sca-1 (*Ly6a*) is marker often used to identify hematopoietic stem cells, and a mixture of stem, progenitor, and a few differentiated cell types in some organs[15]. It is an 18-kDa protein with a glycosylphosphatidylinositol (GPI) anchor to the cell plasma membrane[15]. Sca-1 was originally identified as a cell surface protein upregulated on activated lymphocytes[16]. Sca-1 expression is known to be downregulated as hematopoietic stem cells differentiate into myeloid progenitors, lymphoid progenitors, and are upregulated when differentiating into culture colony forming unit progenitors, prothymocytes, and lymphocytes[15]. Presently, the role and function of Sca-1 is unknown. It is believed that the glycosylphosphatidylinositol-anchored proteins (GPI-APs) are involved with cell-cell adhesion and signaling[15]. However, downstream pathways are yet to be elucidated. Importantly, Sca-1 is commonly found in murine species; however, a human ortholog for this marker has not yet been identified[17]. Human homologs for the murine *Ly6* family of proteins have been identified[15]. Therefore, it is hypothesized that the role Sca-1 plays in mice may be attributed to other *Ly6* genes or GPI-APs in humans. Sca-1^+ has been identified on cells that have the potential to become adipocytes, smooth muscle cells, hepatocytes, epithelial cells, and more, in various organs, including the liver, prostate, mammary gland, dermis, musculoskeletal system, and notably the cardiovascular system[15].

In the heart, Sca-1$^+$ cells have been shown to play a regenerative role following myocardial infarction (MI)[18]. In that study, the authors attributed the attenuation of functional remodeling in response to the MI to paracrine-mediated angiogenesis[18]. Therefore, it calls into question the identity and function that cardiac resident Sca-1$^+$ cells play in naïve and pathological conditions.

C-kit, or cluster of differentiation 117 (CD117), is a type 3 receptor tyrosine kinase (RTK) receptor. The protein structure of this receptor includes 5 immunoglobulin extracellular domains, a transmembrane region, two intracellular kinase domains separated by a kinase insert sequence, and a carboxy-terminal[19]. It binds to a stem cell factor (SCF), commonly referred to as "c-kit ligand", resulting in intracellular signal transduction. Signal transduction involves autophosphorylation, causing signaling proteins such as Src homology 2, to bind to phosphorylated tyrosine residues in the intracellular region[19]. The c-kit receptor is involved with multiple pathways such as the phosphatidylinositol-3'-kinase (PI3K) pathway (cell metabolism, growth, proliferation, survival)[20], the Src family kinase pathway (proliferation, adhesion, migration)[21], the mitogen-activated protein kinase (MAPK) pathway (proliferation, differentiation, development, inflammatory response, apoptosis)[22], and the phospholipase C and D pathways[19]. SCF binding to c-kit is crucial for cell maintenance, including hematopoiesis, and in the reproductive tract, intestine, and nervous system, as this protein is found on hematopoietic cells, germ cells, melanoblasts, interstitial cells of Cajal, and others[19]. C-kit is also shown to play a role in vasculogenesis in pathological conditions, through cell mobilization from chemokines and cytokines[23]. C-kit is often used as a hematopoietic stem cell marker, and importantly, is present in

humans[19]. Therefore, research using the c-kit marker has direct implications for human physiological and pathological conditions.

1.1.3 Cardiac resident Sca-1$^+$ cells and c-kit$^+$ cells

Various types of cell populations exist within the heart, including cardiomyocytes, fibroblasts, endothelial cells, pericytes, leukocytes, and other smaller cell populations[24]. The heart is known to have populations of cells that express the cell surface markers for stem cells, Sca-1 or c-kit.

The exact nature of cardiac Sca-1$^+$ cells and c-kit$^+$ cells is unclear. It was originally believed that these cells had the ability to differentiate into cardiomyocytes and could contribute to repair and regeneration of injured myocardium. Many independent groups were able to show a beneficial effect of "cardiac progenitor cell" administration in various animal models, including mice, rats, pigs, and cats[25]. These studies showed attenuated thinning of the left ventricle (LV) wall, reduced scar size, and reduced diastolic and systolic LV volumes[25]. However, in 2010 it was shown that though these cells may improve cardiac function, they fail to engraft and do not differentiate into new cardiomyocytes[26].

In contrast to reports that suggested a cardiomyocyte precursor nature of cardiac Sca-1$^+$ cells and c-kit$^+$ cells, careful analysis in recent studies show that a majority of cardiac c-kit$^+$ cells co-express CD31 and Tie2, which are commonly used to identify endothelial cells[27]. The cells were shown to not co-express α-smooth muscle actin (α-SMA, smooth muscle cell marker), cardiac troponin T (cTnT), or Nkx2.5 (cardiomyocyte markers)[27]. Furthermore, it was shown that a majority of cardiac Sca-1$^+$ cells co-express c-kit (found on stem cells), Tie2, and CD31 (cell surface receptors typically seen on endothelial cells)[28]. These Sca-1$^+$ cells did not co-express cardiac troponin T, or Nkx2.5

(typical cardiomyocyte markers)[28]. One study was able to take a genetic approach to mark the Kit locus and found that c-kit$^+$ cells contribute minimally (0.008%) to the production of new cardiomyocytes[29]. Similarly, another study showed through genetic lineage tracing that Sca-1$^+$ cells contribute to a "physiologically insufficient" level of cardiomyocyte generation[30]. Together, the recent evidence now suggests that cardiac resident Sca-1$^+$ cells and c-kit$^+$ cells may be endothelial precursor/progenitor cells. Importantly, to the best of our knowledge, studies have not yet investigated the endothelial functional characteristics of these cells, nor have these studies used a global approach to look at the characteristics of cells from the entire heart. Further studies are needed to better characterize the cardiac resident Sca-1$^+$ cells and c-kit$^+$ cells.

1.1.4 Characteristics of Endothelial Cells

The endothelium is a layer of tissue that lines blood vessels and consists of endothelial cells (ECs) connected by tight junctions[31]. These cells are involved in forming a barrier between blood and the basement membrane of blood vessels[32], regulation of blood pressure[33], platelet adhesion[34], and angiogenesis (formation of new blood vessels)[35]. ECs can be identified through their cobblestone morphology and expression of cell surface markers, as well as their specific functions: acetylated low-density lipoprotein (AcLDL) uptake, lectin-binding, and network/tube-formation (*in vitro* and *in vivo*).

ECs from various types of blood vessels, when isolated and cultured *in vitro*, show a typical cobblestone-like morphology[36]. These cells are plastic adherent and do not require support matrix for culture. In addition, the characteristics of ECs include expression of specific cell surface markers. The most widely used cell surface marker for endothelial cells is the cluster of differentiation 31 (CD31, or platelet endothelial cell adhesion

molecule-1; PECAM-1), which is a cell surface protein highly expressed on endothelial cells[37]. Low expression of CD31 can also be found on platelets and leukocytes[37]. The protein is 130kDa, and contains an extracellular site, immunoglobulin domains, transmembrane domain, as well as a cytoplasmic tail[38]. The extracellular site contains a homophilic cell adhesion site, which enables firm endothelial cell-to-cell adhesion, used to create a barrier to line blood vessels. The cytoplasmic tail contains immunotyrosine-based inhibitory motifs that, when activated by Src homology phosphatases, increase cell motility and adhesion, as well as cytoprotection[37]. CD31 is a well-established marker used to identify cells of endothelial characteristics, and together with markers of stem cells, it has been widely used to identify endothelial stem/progenitor cells in various tissues[39].

Functional characteristics of ECs include acetylated low-density lipoprotein (AcLDL) uptake, lectin binding, network formation when cultured on extracellular matrix gel, and production of nitric oxide (NO). Ac-LDL is a carrier protein that facilitates the movement of cholesterols throughout the body. ECs have the ability to take-up AcLDL through a scavenger pathway[40,41]. These cells display CD36, a class B scavenger receptor, that facilitates the uptake and degradation of the lipoprotein[42]. This may result in physiological consequences for endothelial tissue, such as the removal of modified lipoproteins (such as cholesterol) from the blood[43], endothelial nitric oxide synthase (eNOS) generation of superoxide anion[44], and has also been implicated as having a role in atherosclerosis[43]. As a result, the addition of a fluorescently labeled AcLDL to culture media of cells is often used to identify and characterize ECs[40]. Another characteristic of ECs is that lectins, proteins that bind to carbohydrates, bind to the glycocalyx on the EC membrane. The endothelial glycocalyx is a brush-like structure comprised of glycoproteins

on the inner lining of microvasculature. A healthy endothelial glycocalyx forms a repulsive barrier between the blood within the vessels and the vessel wall. Griffonia simplicifolia-1 (GS-1) lectin can bind to alpha-D-galactosyl residues in the glycocalyx surrounding endothelial cells[45]. Therefore, the addition of a fluorophore to GS-1 lectin can be used to identify and characterize ECs. Another characteristic of ECs is to form tube-like structures or networks, when cultured on gelled extracellular matrix such as fibrin or collagen gel, Matrigel, Geltrex, and Cultrex. Matrigel is an extracellular matrix protein, created from Engelbreth-Helm-Swarm mouse sarcomas[46]. Commercialized Matrigel can vary[47]; however, it generally consists of a mixture of basement membrane proteins such as laminin, entactin, type IV collagen, and proteoheparan sulfate[48]. It is commonly used as a basement substance to allow the growth of certain specialized cells or organoid tissues[49] and to assess the *in vitro* (network- or tube-formation) and *in vivo* angiogenic potential of ECs. Network formation can be used as an *in vitro* functional assay of the vasculogenic ability of ECs[50].

1.1.5 Endothelial Progenitor Cells

Endothelial progenitor cells (EPC) are unipotent cells (progenitors) that are committed to the endothelial lineage. These cells were originally discovered in the late 1990's, from human mononuclear blood cells[51]. These circulating EPCs were shown to express CD34 (found on hematopoietic stem cells), along with CD31, VEGFR2, and Tie2 (endothelial cell markers)[51]. EPCs are known to have a role in endothelial regeneration[52]. EPCs also play a role in neovascularization, as these cells incorporate into sites of active angiogenesis[51]. These cells were also shown to have physiological relevance in tissue repair and vascular regeneration, and to have therapeutic potential[53]. One study was able to show lower levels of circulating EPCs in response to ischemic cardiomyopathy[54]. Another

showed that patients at higher cardiac risk expressed less EPC colonies, as well as more senescent EPCs[55]. Furthermore, these cells were shown to proliferate and mobilize in response to ischemic injury[56] and an association between increased circulating EPCs and decreased risk of death from cardiovascular outcomes has been reported[57]. In addition, several studies have shown therapeutic importance of circulating EPCs in various diseases including peripheral arterial disease[58,59], coronary artery disease[60], and pulmonary hypertension[61].

Characterizing cells as EPCs remains ambiguous. There are currently no known specific markers for EPCs, as common markers found are also expressed by vascular endothelial cells[62]. Working definitions of EPCs often use the combination of CD31 expression, AcLDL uptake, and lectin binding. However, some monocyte populations are known to express endothelial cell marker CD31, and macrophages are known to uptake LDL[63] and bind to lectin[64]. Other markers, such as CD133 (found on hematopoietic stem cells and endothelial progenitor cells) may be used to further characterize these cells. However, this marker is known to give rise to populations that differentiate into endothelium or remain hematopoietic[65]. These obstacles present difficulties in characterizing cells as EPCs. Varying nomenclature further confounds the identity and functions of these cells; common terminology includes “early and late EPCs” “circulating angiogenic cells” (CACs), and “endothelial outgrowth cells”. It remains ambiguous whether these characterizations describe the same cell population. For example, one study showed significant differences in “early EPCs” compared to “late EPCs” in their endothelial characteristics, including network formation, morphology, and even nitric oxide production[66]. The literature also describes commercially available kits to count

endothelial cell colony-forming units (CFU-ECs) as EPCs, however some data shows that despite similar nomenclature, these are not the same type of cell[67]. As a result, EPCs are loosely defined by "an endothelial cell phenotype, significant proliferative potential, and the capacity to self-assemble into functional blood vessels *in vivo*"[68].

1.1.6 Sex Differences in Endothelial Progenitor Cells

Biological sex influences the survival, proliferation, function, and pluripotency of various stem cell types[69,70]. A study showed more circulating EPCs in normotensive and pre-hypertensive premenopausal women compared to age-matched men[71]. Varying levels of circulating EPCs were also seen throughout the menstrual cycle[72,73]. Sex differences in the abundance of these cells tend to show the female sex is associated with a higher abundance of these cells[74]. In addition, some studies have shown the role of sex hormones in EPCs function. Estrogen may reduce EPCs senescence through telomerase activity[75], and along with progesterone, may increase EPC proliferation[76]. Estrogen treatment of these stem cells was also shown to improve myocardial function when infused into mouse hearts after acute ischemia[77]. Another study showed that when mice were induced to have an MI, there were higher levels of circulating EPCs in ovariectomized estradiol treated mice, which was attenuated in eNOS deficient mice[78]. Estradiol was also shown to stimulate capillary formation using EPCs, through the ER-α pathway[79]. Moreover, the other female sex hormone progesterone was shown to increase viability of EPCs[80]. Overall, early evidence shows the ability of biological sex and sex hormones to affect EPC abundance, survival, proliferation, and function.

1.2 Right-sided Heart Failure

1.2.1 General Introduction to Right-sided Heart Failure

Right(-sided) heart failure (RHF) is characterized by the inability of the right ventricle (RV) to pump an adequate amount of blood into the lungs and maintain cardiac output. This may be due to decreased RV function leading to insufficient blood flow and/or elevated filling pressures. RHF is associated with poor prognoses in various cardiopulmonary disorders[81]. For example, in patients with heart failure with preserved ejection fraction (HFpEF), many have markers of RV dysfunction such as abnormal tricuspid annular plane systolic excursion (TAPSE), reduced RV fractional area change, and RV hypertrophy/remodeling, and are more likely to have atrial fibrillation, pacemakers, and chronic diuretic therapy[82,83]. In left-sided heart failure (LHF) patients, 20-50% of those with preserved ejection fraction (HFpEF), and 50-70% of those with reduced ejection fraction (HFrEF), demonstrate RV dysfunction[84,85,86,87]. Importantly, RV function is a strong predictor of survival in patients with pulmonary artery hypertension (PAH)[88]. Therefore, maintaining RV function and preventing the development of RHF remains an important objective in clinical research.

1.2.2 Current Therapies for Right Heart Failure

Current therapies for RHF are limited. Conventional therapies look at reducing RV afterload. This is through the use of medications, such as: prostacyclin analogs, PDE inhibitors and activators of guanalyl cyclase, and nitric oxide pathways, to induce vasodilation of the pulmonary artery (PA)[89]. However, these interventions target vasculature, and do not provide direct benefits to the pathologically remodeled RV[88]. Other conventional treatments involve preload reduction by using diuretics; however, this only

provides symptomatic relief[89]. Many evolving therapies targeting RHF were developed and proven to be beneficial for the LV yet are not effective for the RV. For example, in a study in which Wistar rats were subjected to pulmonary trunk banding surgery, bisoprolol and losartan lowered heart rate and mean arterial pressure; however, did not improve RV function, or decelerate RV hypertrophy compared to healthy controls[90]. Another study found that eplerenone (an inhibitor of aldosterone, and the renin-angiotensin-aldosterone system, RAAS), when used in combination with losartan, did not affect RV failure in a rat pulmonary artery banding model of RV overload[91]. The use of therapies developed for the LV on RV pathology is due to a misconception of the similarities between the two tissues; however, the ventricles demonstrate clear differences. Ventricular differences include embryological origins, perfusion of myocardium during the cardiac cycle (RV supplied in systole, LV supplied in diastole), loading conditions, resistance to blood ejection, afterload, and differences in angiogenesis in response to stress (an immediate decrease in capillary density in response to stress in the RV)[92]. This highlights the need for therapies specifically targeting RV function after adverse remodeling in pathological conditions such as RV overload.

1.2.3 Models of Right Heart Failure used in Research

RHF is often studied using models of severe pulmonary hypertension (PH). PH is a disease in which the pulmonary vasculature experiences an elevation in pressure. This causes an increase in afterload that the RV must overcome to pump blood into the lungs for oxygenation. Therefore, when PH is severe and chronic, it leads to RV remodeling and ultimately to RHF. RHF associated with PH can be investigated using various animal models.

Compared to other models of RV overload, the monocrotaline model of PH is a less resource intensive way to induce RV remodeling. Monocrotaline (MCT) is a plant-derived pyrrolizidine alkaloid that is metabolized in the liver with cytochrome P450 into monocrotaline pyrrole (MCT-P) and transported to the lungs, where it interacts with PA endothelial cells to induce damage[93]. The exact toxicological mechanism by which MCT induces endothelial cell injury specific to the PA remains unknown, although some point to an affection on calcium sensitive receptors[94]. The destruction of endothelial cells in the pulmonary artery results in an increased pressure in the pulmonary vasculature, which leads to PH and eventually RHF. The MCT model is widely used in research for its feasibility, as the animals are injected with MCT and observed over time for the progression of the disease. However, many point towards liver toxicity, and myocarditis associated with MCT as confounding variables, as these do not occur in other models of PH and RHF[95,96]. The MCT model of PH remains favourable in the eyes of many researchers; however, the conclusions drawn from these studies must be carefully extrapolated when looking at applications for therapeutic potential.

The Sugen hypoxia (SUHx) model of PH involves an injection of SU5416 followed by exposure of animals to chronic hypoxic (10% oxygen) conditions. SU5416 is a vascular endothelial growth factor receptor (VEGFR) antagonist, and this pathway normally plays a role in EC survival and the formation of blood vessels by altering cell migration, proliferation, and survival[97]. In SUHx model, SU5416 injection leads to EC apoptosis in the lungs and combination of EC apoptosis and hypoxia leads to severe progressive PH[98]. The SUHx model reproduces several key pathological features of human PH including sustained elevation in mean pulmonary artery pressure, appearance of plexiform-like

lesions (hallmark of human PH), severe RV remodeling, and development of RHF[99]. This model is more resource intensive than the MCT model, as it involves the maintenance of the animal in hypoxic conditions after the SU5416 is administered. Some authors report increased lung emphysema, but this may only be in certain strains of rats used[99].

The pulmonary artery banding (PAB) model is a model to recapitulate RV remodeling and RHF. This model involves surgically opening the chest and inserting a tensile band over the pulmonary artery[100]. The PAB model is known for its technical difficulty, as the size of the pulmonary artery depends on the animal model being used. This model also leads to RV remodeling independent of effects on pulmonary vasculature[101]. However, some argue that this model does not demonstrate how the disease develops chronically, as the band is inserted to immediately increase pressure in the pulmonary artery. Therefore, this model may be helpful to directly assess the consequences of an increased pressure of the pulmonary artery, but abrupt change in pressure should be taken into consideration in interpretation of results.

In preclinical models, the animal species and strains used could have influence on the outcome. For example, marked strain-specific differences have been reported in the SUHx model[98]. The most common strain of rat used for research is the Sprague Dawley (SD) rat. SD rats are an outbred albino rat strain, originally developed by breeding Wistar rats with hybrids of wild and laboratory stocks[102]. As these rats are outbred, there may be genetic variability when used for research purposes. For example, one study showed phenotypic differences including differences in body fat mass, gross liver weight, testicular weight, and cholesterol levels, when comparing Charles River Laboratory SD rats compared to Harlan SD rats[102]. The authors hypothesize that this may represent a research

variable impacting future studies. To mitigate this, an inbred strain of rat may provide clearer research insights. Fischer CDF rats are an inbred albino rat strain, developed at the National Institute of Health in 1992. These rats were adopted by Charles River Laboratories in 1996. A study conducted in 2018 showed strain differences while investigating RV remodeling between SD and Fischer CDF rats[103]. Harlan SD rats were shown to have an adaptive remodeling response (higher survival rate, less RV dilation, less reduced cardiac output, and preserved RV ejection fraction) when exposed to SUHx, while Fischer CDF rats exhibited decreased cardiac output, RV ejection fraction, increased RV dilation, decreased angiogenic gene expression, and a greater reduction in capillary density[103]. The mechanism of differential angiogenic response between the two strains remain unclear, and warrants further study considering the role capillary density may play in adaptive and maladaptive remodeling. The use of Fischer CDF rats in physiological and pathological RV conditions may provide us with more insight in adaptive and maladaptive RV remodeling. Furthermore, understanding the differences between these two rat strains could uncover novel targets for prevention and/or treatment of RHF.

1.2.4 Mechanisms of Right Heart Failure

Angiogenesis has an important role in the maintenance of RV function in models and in patients with increased RV afterload. For example, one study showed RV angiogenesis as an early adaptive response in a chronic hypoxia model of RV overload[104]. Mice subjected to chronic hypoxia for 3 weeks showed increased capillary length, surface area, volume, as well as increased RV endothelial cell proliferation[104]. Similarly, decreased angiogenesis has also been shown to cause RHF. One study using human RV free wall patient samples found that those with decompensated RV failure demonstrated a decreased

capillary density compared to patients with a compensated RV[105]. Furthermore, the study reported that decreased miR-126 expression, decreased phosphorylated extracellular signal-regulated kinases (p-ERK), and vascular endothelial growth factor (VEGF) receptor signaling in EC obtained from decompensated RV[105]. Together, the study demonstrated that lack of angiogenesis during RV remodeling can lead to decompensated RVs[105]. Decreased angiogenesis has been further studied using rat models of RV overload. One study noted decreased capillary density and volume in a Fischer CDF rat strain, which was associated with maladaptive RV remodeling and RHF[103]. Endothelial cells are primarily responsible for the formation of new vessels, therefore the investigation of endothelial and endothelial-like cells from the heart may allow us to further understand various cardiac pathologies.

Increased fibrosis can be seen in RHF. One study using patient sample data found increased fibrosis in those with PH-HFpEF[106]. However, it is important to note that fibrosis may not be the prevailing mechanism behind RHF. One study was able to show rats subjected to pulmonary trunk banding procedure and treated with the anti-fibrotic agent pirfenidone, still developed RV failure, and hemodynamic measurements declined[107]. Another study was able to show that fibrotic signaling or fibrosis was not seen in the transition from compensated to decompensated RV dysfunction using a rat model of RV overload[108]. Therefore, fibrosis has been suggested as one possible mechanism for RHF by several studies but may not be the primary mechanism by which this pathology develops.

Shifts in metabolism and oxidative stress are also seen in cases of RHF. For example, in a patient that died of RV failure, there was an increase in GLUT1 and PDK4, which are glycolytic markers, showing a shift from an oxidative state to a more glycolytic

metabolism, compared to the control group[109]. Another study was able to note that the use of dichloroacetate (an inhibitor of pyruvate dehydrogenase kinase, which itself inactivates pyruvate dehydrogenase), increased glucose oxidation and RV function in MCT injected rats[110]. Furthermore, higher oxidative stress is seen in those with PH. In human lung tissue with idiopathic PH, there was reduced superoxide dismutase (an antioxidant), and high oxidant stress markers[111]. In a rat model of SUHx, the failing right ventricle contained less heme oxygenase-1 (antioxidant) expression[111]. Therefore, in both patient samples and models of RHF, shifts in metabolism favouring glycolysis, is associated with oxidative stress.

Inflammation and the involvement of the immune system has also been implicated in the development of RHF. For example, circulating inflammatory markers such as IL-1β, IL-6, TNF-α, were shown to be increased in patients with PH[112]. Inflammation in the RV itself is observed. One study noted in a rat MCT model of RHF, showed increased mRNA expression of TNF-α, and immunohistochemistry showed increased staining of myeloperoxidase (MPO, marker of neutrophil activity)[113]. Similarly, another study noted increased pro-inflammatory cytokines such as IL-1α, IL-1β, TNF-α in the RV of pigs subjected to surgical anastomoses of left innominate artery to the pulmonary arterial trunk[114]. Increased circulating inflammatory markers, as well as inflammatory markers seen in the RV are both seen in RHF.

Decreased angiogenesis, increased fibrosis, metabolic shift favouring glycolysis, oxidative stress and inflammation are all seen in both patient data and models of RHF. Though all mechanisms have been shown to be involved in the progression of RHF, angiogenesis seems to be a key mechanism by which these diseases progress, therefore the

role of endothelial and endothelial-like cells in angiogenesis may provide us with clear and direct insights for RHF.

1.2.5 Sex Differences in Right Heart Failure

The female RV is shown to be more resilient to stress compared to the male RV. One study was able to show a relationship between testosterone and survival outcomes, by comparing PAB castrated mice to PAB controls. Testosterone levels correlated to hemodynamic measures and was associated with increased cardiomyocyte size and fibrosis[115]. With increased cardiomyocyte size, the existing capillary density may not be sufficient to provide adequate blood supply. Rats injected with MCT resisted RV dysfunction by echocardiographic and hemodynamic measurements, when treated with estradiol[116]. Estrogen attenuated the loss of mitochondrial density in SUHx treated mice, with higher mitochondrial quality and oxidative capacity in these mice compared to mice not treated with estrogen pellets[117]. Athymic male mice injected with Sugen demonstrated increased pulmonary artery muscularization, and increased cardiomyocyte area[118]. From this, it is clear that sex differences may exist in the progression of RHF and RV remodeling. It is not yet well described how sex differences influence endothelial and endothelial-like cells in RV pathology.

1.3 Rationale

Sca-1$^+$ cells and c-kit$^+$ cells were at one time purported to be cardiomyocyte progenitor cells, though more recent evidence better clarifies them as only endothelial precursor/progenitor cells. Flow cytometry of the entire heart offers quantitative information on cellular identity with greater accuracy than sectioning. Using SD rats to isolate and perform *in vitro* functional assessment of these cells, this may further elucidate more of the characteristics of these cells. To date research attention for these cells have focused on the LV not the RV as an independent variable. Furthermore, sex differences appear in cardiac right-sided pathologies, as well as in the effect of sex hormones on other stem cell populations. Interestingly, isolated tissues obtained from heart surgery were able to show more c-kit$^+$ cells produced by females compared to males[72]. Therefore, it would be of interest to compare abundance and function of cardiac c-kit$^+$ cells and Sca-1$^+$ cells in males and females. Strain-specific differences in rat models of cardiopulmonary diseases have been reported therefore the use of SD and Fischer CDF rat strains would be relevant. Understanding the nature and function of these cells in baseline and pathological PH conditions leading to RV remodeling, will lead to a more comprehensive understanding of cardiac physiology, and may help in understanding their relevance. Therefore, this project aims to better understand the nature and function of cardiac Sca-1$^+$ cells and c-kit$^+$ cells, and investigate differences in these cells across ventricles, sexes, rat strains, and in pathological RV remodeling.

1.3.1 Hypothesis

We hypothesized that cardiac resident Sca-1$^+$ cells and c-kit$^+$ cells are cardiac EPCs (CEPCs) with angiogenic function. Biological sex, genetic background, and disease state

influence the abundance or function of these cells.

1.3.2 Major Objectives

1. To further investigate the endothelial characteristics of cardiac resident Sca-1$^+$ cells and c-kit$^+$ cells through cell surface receptor expression, morphology, and functional assays.
2. To investigate the differences in the abundance of these cells between the LV and septum (LV+S), and RV
3. To investigate sex differences in the abundance of these cells in healthy SD rats.
4. To investigate strain differences in the abundance of these cells in healthy SD and Fischer CDF rats.
5. To determine the effect of RV pressure overload on the abundance of these cells and assess sex differences in changes in abundance of these cells.

CHAPTER 2. MATERIALS AND METHODS

2.1 Antibodies

Antibodies were used for flow cytometry and magnetic sorting of cells. Antibodies for endothelial cells include mouse anti-rat CD31 conjugated to eFluor 660 (Invitrogen, CA, USA; Catalogue #50-0310-82), and mouse anti-rat CD31 (Millipore, MA, USA; Catalogue #MAB13937). Cell surface markers include rabbit anti-rat Sca-1 (Millipore, MA, USA; Catalogue #AB4336), and rabbit anti-rat C-kit/CD117 (MyBioSource, CA, USA; Catalogue # MBS555311). Secondary antibodies include anti-rabbit Alexa Fluor 488 (Invitrogen, CA, USA; Catalogue #A27034). Mouse IgG1 kappa isotype control (Clone P3.6.2.8.1) was used (Invitrogen, CA, USA; Catalogue #50-4714-80). Secondary magnetic beads used for magnetic sorting include goat anti-rabbit IgG microbeads (Miltenyi, Begisch Gladbach, Germany, Catalogue #130-048-602), and goat anti-mouse IgG microbeads (Miltenyi, Begisch Gladbach, Germany, Catalogue #130-048-401).

2.2 Animal Handling and Ethics Statement

All animal procedures were approved by the Dalhousie University committee on laboratory animals and were in accordance with the Canadian council on animal care guidelines. SD and Fischer CDF rats, aged 6-8 weeks of age, were obtained from Charles River Laboratory (Montreal, QC, Canada) and were allowed one week acclimatization before any procedure. All rats were housed in the Carlton animal care facility at Dalhousie University. Throughout the experiments, all rats were maintained on light-dark (12 hours/12 hours) cycle and had access to food water *ad libitum.*

2.3 Rat Heart Extraction and Tissue Digestion

SD and Fischer CDF rats were anesthetized using isofluorane (5%, 2L/min) and surgical plane anesthesia was confirmed by toe pinch. Upon confirmation of surgical plane

anesthesia, the abdominal cavity was opened and rats were sacrificed by exsanguination. Following sacrifice, the thoracic cavity was opened, hearts were excised, and placed in endothelial growth media 2 (Lonza, MA, USA; Catalogue #CC-3129, #CC-4176) with 2% charcoal-stripped fetal bovine serum to prevent the addition of sex hormones in culturing conditions (CS-FBS; Sigma-Aldrich, MO, USA; Catalogue #F6765) for transport. Hearts were washed with Ca^{2+}/Mg^{2+} free phosphate-buffered saline (PBS) (Gibco, CA, USA; Catalogue #10010023) and placed on a petri dish for tissue separation. Fat tissue, blood vessels, valves, and atria were removed, and the LV+S was separated from the RV. Fulton Index (FI) was calculated as the RV mass divided by LV+S mass (RV/LV+S)[119]. Then, the LV and RV were minced using surgical scissors, and digested enzymatically using collagenase-dispase (Roche Diagnostics, NC, USA; Catalogue #11097113001). Ventricular tissue was then pipetted into a 50mL collection tube containing fresh collagenase-dispase (1mL per 75-100mg heart tissue). Tubes were placed in a water bath at 37°C for 15 minutes. The tissue was then passed through a 40μm cell strainer (Corning, NC, USA; Catalogue #352340), and remaining tissue was placed into a tube with fresh collagenase-dispase for incubation with the enzyme in a water bath at 37°C for an additional 15 minutes. Following the second digestion, the cell suspension was passed through a 40μm cell strainer. The single cell suspensions were then centrifuged at 400g for 5 minutes. Supernatants were discarded and pellets were re-suspended in flow buffer containing 3% BSA in PBS for flow cytometry experiments. Cells were re-suspended in de-gassed magnetic sorting buffer containing 0.5% BSA and EDTA in PBS for magnetic sorting experiments.

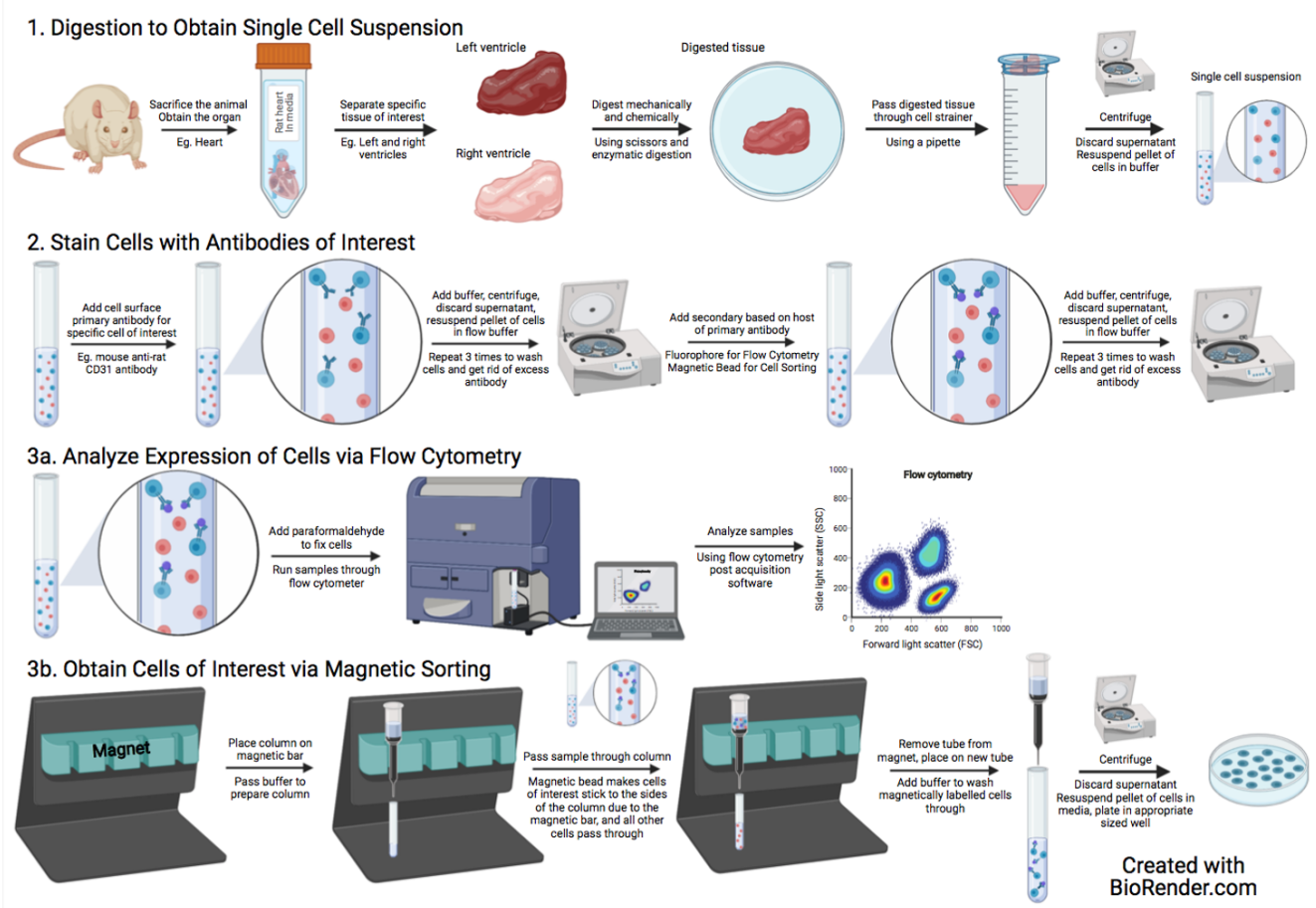

Figure 1. Identification of cardiac resident Sca-1$^+$ cells and c-kit$^+$ cells through flow cytometry, and isolation through magnetic sorting. Flow chart describing methodology used to identify cell surface receptors through flow cytometry, and isolation of cardiac resident Sca-1$^+$ cells through magnetic sorting, used for AcLDL uptake and lectin binding assay, matrigel, and long-term culture.

2.4 Cell Staining for Flow Cytometry

The resultant cell suspension was divided into seven round bottom polystyrene tubes, and re-suspended in buffer to create a final volume of 100 μL. Primary antibodies were added into the various tubes, including mouse anti-rat CD31 conjugated to eFluor 660 (1:50) (Invitrogen, CA, USA; Catalogue #50-0310-82), rabbit anti-rat Sca-1 (1:50) (Millipore, MA, USA; Catalogue #AB4336), and rabbit anti-rat c-kit/CD117 (1:50) (MyBioSource, CA, USA; Catalogue # MBS555311) for flow cytometry. Cell suspensions were incubated in the dark at 4°C for 30 minutes. A wash step was performed by adding 1 mL of flow buffer, centrifugation at 400 g for 5 minutes, removal of supernatants, and re-suspension. The wash step was repeated three times and cells were re-suspended in in 100 μL flow buffer after the last wash. Secondary antibodies and IgG isotype controls were added (1:333) and incubated in the dark at 4°C for 30 minutes. The wash step was then again repeated three times. Cells were resuspended in 100 μL flow buffer and fixed by adding 400 μL 4% paraformaldehyde (PFA) and stored at 4°C in PFA until flow cytometry analysis (within 5 days post fixation).

2.5 Flow Cytometry

Cell surface markers were analyzed using BD FACS Celesta (BD Biosciences, MA, USA) with FACS Diva (BD Biosciences, MA, USA) at the Flow Cytometry CORE facility, Dalhousie University. Forward scatter (FSC) and side scatter (SSC) voltages were set at 655 V and 405 V respectively. Forward scatter area (FSC-A) and side scatter area (SSC-A) were used to discriminate debris from the cell population. SSC-A and SSC-H were used for doublet discrimination. Voltages were set as follows for fluorophores: eFluor660 at 500 V, and AF488 at 460 V. Flow cytometry data was analyzed using FlowJo post-acquisition

software (BD Biosciences) (Figure 2). Live population of cells were gated using FSC against SSC. Doublet discrimination was performed by plotting FSC-Area against FSC-Height. Plots were gated using blank samples to identify autofluorescence, and IgG Isotype controls and secondary only samples to distinguish non-specific binding.

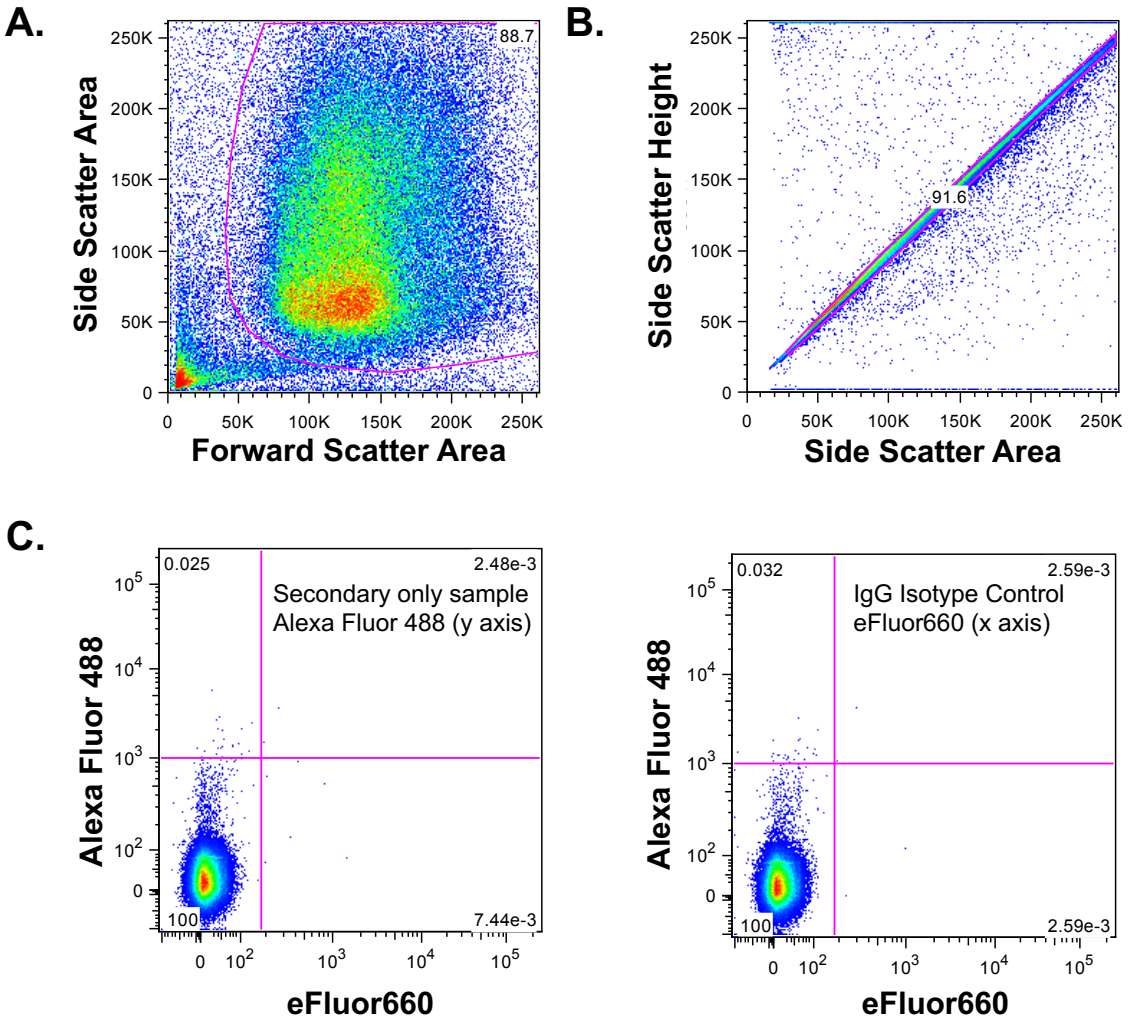

Figure 2. Representative images showing gating technique for flow cytometry.
A. Forward scatter-area plotted against side scatter-area to identify live cell population. B. Side scatter-area plotted against side scatter-height to identify single cells. C. Representative flow cytometry data for secondary antibody only (goat anti-rabbit Alexa Fluor 488) or for isotype control (eFluor660) and quadrant style gating. Individual secondary antibody only and isotype control samples used for each sample type, and each experiment (male LV, male RV, female LV, female RV).

2.6 Cell Sorting

Cells were magnetically sorted using an OctoMACS Separator (Miltenyi Biotec, Begisch Gladbach, Germany, Catalogue #130-042-108). Briefly, separation columns were placed on the magnet, and conditioned with 500 µL of de-gassed magnetic buffer solution, to prevent obstruction of the column. Solution was de-gassed by applying vacuum pressure for at least 1 hour. Single-cell suspensions were re-suspended to create a final volume of 300 µL and incubated with mouse anti-rat CD31 (1:20) (Millipore, MA, USA; Catalogue #MAB13937), and rabbit anti-rat Sca-1 (1:50) (Millipore, MA, USA; Catalogue #AB4336) at 4°C for 30 minutes. The wash step was performed three times, before secondary antibodies were added. Initially, goat anti-rabbit magnetic beads (1:5) (Miltenyi, Germany, Catalogue #130-048-602) were used to sort and obtain Sca-1^+ cells. The wash step was performed three times, using magnetic sorting buffer, after the completion of incubation with magnetic beads. Cell suspensions were applied to magnetic columns and washed with aliquots of de-gassed magnetic buffer. The columns were then removed from the magnet, and cells labeled with the magnetic beads were eluted using magnetic sorting buffer. Cells were washed and re-suspended in EGM-2MV (Lonza, MA, USA; Catalogue #CC-3129, #CC-4147) + 5% CS-FBS (Sigma-Aldrich, MO, USA; Catalogue #F6765). Cells were then plated in wells coated with human plasma fibronectin (Gibco, CA, USA; Catalogue #33010-018). Fibronectin was prepared by reconstituting 5 mg with 5 mL of sterile water. 50 µL of the 1 mg/mL stock solution was further diluted to 10 µg/mL with sterile PBS (Gibco, CA, USA; Catalogue #10010023), before adding to plates. 300 µL was added into each well of a 24-well plate, and incubated at 37°C and 5% CO_2 for 30 minutes. Plates were washed with PBS (Gibco, CA, USA; Catalogue #10010023) before media and cells

were plated. After sorting of Sca-1^+ cells, goat anti-mouse magnetic beads (1:5) (Miltenyi, Germany, Catalogue #130-048-401) were used to sort and obtain $CD31^+$ cells and these cells were cultured under identical condition to Sca-1^+ cells.

2.7 Acetylated Low-Density Lipoprotein (Ac-LDL) and Lectin Binding Assay

Cells were plated into 4 well chamber slides (Thermo Fisher Scientific, NY, USA; Catalogue #154453) coated with fibronectin (Gibco, CA, USA; Catalogue #33010-018), and left to attach overnight in EGM-2MV media. Cells were then washed with PBS, and incubated with DiI AcLDL (1:50) (Invitrogen, Eugene, Oregon, Catalogue #L3484) in EGM-2MV (Lonza, MA, USA; Catalogue #CC-3129, #CC-4147) + 5% CS-FBS (Sigma-Aldrich, MO, USA; Catalogue #F6765) at 37°C and 5% CO_2 for three hours. Then, the cells were washed with PBS and fixed with 4% PFA for 20 minutes. Following Ac-LDL uptake, cells were washed and blocked with 1% BSA in PBS for 20 minutes. Lectin-FITC (1:100) (Invitrogen, ORE, USA; Catalogue #L21415) was added to each chamber of the chambered slide and incubated at room temperature for two hours. Cells were then washed, and the chambers were removed. Slides were then sealed in mounting media with DAPI (ibidi, WI, USA; Catalogue # 50011) and preserved at 4°C in the dark until analysis. Images were taken at 10x, 20x, and 40x on a confocal microscope. Cells were counted using DAPI nuclear stain (blue) to assess number of cells with nuclei per field of view. Quantification of AcLDL uptake was conducted by determining number of DAPI positive cells that demonstrated red "dots" or points (Figure 3A-B). Quantification of lectin binding was conducted by determining number of DAPI positive cells that demonstrated green surrounding DAPI stain (Figure 3A-B). Percentage of cells demonstrating AcLDL uptake

and lectin binding was determined using number of (AcLDL or lectin) positive cells/total number of DAPI positive cells.

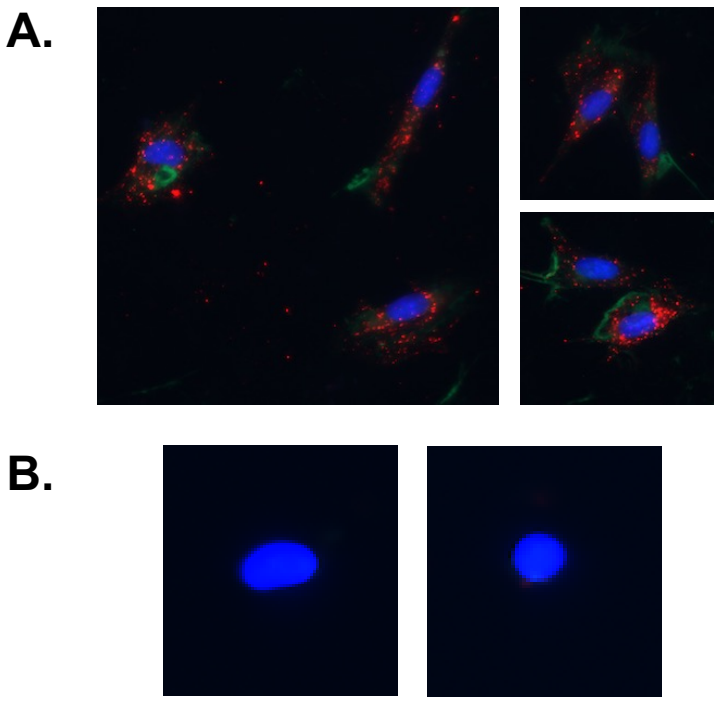

Figure 3. Quantification of AcLDL uptake and GS-1 lectin binding assays. A. Representative images showing cells identified through DAPI nuclear stain (blue) positive for AcLDL (red) uptake and GS-1 lectin (green) binding. B. Representative images showing cells cells identified through DAPI nuclear stain (blue) negative for AcLDL (red) uptake and GS-1 lectin (green) binding.

2.8 Matrigel Network Formation Assay

Matrigel (Corning, NC, USA; Catalogue #356231) was thawed overnight at 4°C and 10 µL of Matrigel was added to each well of an angiogenic slide (ibidi, WI, USA; Catalogue #81506). Slides were incubated for 30 minutes at 37°C and 5% CO_2 to allow Matrigel to gel. $Sca1^+$ cells were isolated by magnetic sorting and plated on the Matrigel. Isolated cells were plated in each well with EBM (Lonza, MA, USA; Catalogue #CC-3129, #CC-4147) and 0.5% CS-FBS (Sigma-Aldrich, MO, USA; Catalogue #F6765). 0, 8, 18, and 24 hour photos were taken on a light microscope at 4x and 10x.

2.9 Long-term Culture of Sca-1^+ Cells and $CD31^+$ Cells

Isolated cardiac $CD31^+$ cells, and Sca-1^+ cells were plated in 24-well plates coated with fibronecin (Gibco, CA, USA; Catalogue #33010-018), and cultured at 37°C at 5% CO_2 in EGM-2MV (Lonza, MA, USA; Catalogue #CC-3129, #CC-4147) with 5% CS-FBS (Sigma-Aldrich, MO, USA; Catalogue #F6765). Media was changed every 2 days. Cells were passaged when plates reached 70-80% confluency. For passage, cells were washed with warm Ca^{2+}/Mg^{2+} free PBS (Gibco, CA, USA; Catalogue #10010023) and incubated with TrypLE (Gibco, CA, USA; Catalogue #12604021) at 37°C at 5% CO_2 for 5 minutes. Cells were collected in 15 mL tubes and TrypLE (Gibco, CA, USA; Catalogue #12604021) was inactivated by diluting with 2 times volume of Ca^{2+}/Mg^{2+} free PBS (Gibco, CA, USA; Catalogue #10010023). Cells were centrifuged at 400 g at 4°C for 5 minutes. Supernatant was removed and the pellet of cells was re-suspended in appropriate media for testing or culture.

2.10 Monocrotaline Model

MCT (Sigma-Aldrich, St. Louis, Missouri, Catalogue #C2401) was dissolved in

1.0M HCl and the pH was adjusted to 7.4 using 1.0M NaOH. Volume was adjusted using sterile water for injection to obtain 20 mg/kg MCT. Adult male and female Fischer CDF rats were weighed and subcutaneously injected with MCT (60mg/kg). Animals were monitored for four weeks following injection.

2.11 Hemodynamic measurements

Right ventricular systolic pressure (RVSP) was measured using high-fidelity pressure catheters (Transonic-Scisense Inc., ON, Canada) at 4 weeks MCT injection. For RV catheterization, rats were anaesthetized by isoflurane inhalation (Induction: 5% isoflurane at 1 L/min O_2; maintenance: 2% isoflurane at 1 L/min O_2). The pressure catheter was inserted into the right jugular vein and advanced through the superior vena cava and right atrium into the RV. Hemodynamic parameters were recorded and analyzed using the LabScribe3 software (iWorx, Dover, NH, USA).

2.12 Statistical Analysis

Statistical analysis of the data was performed using Student's t-test for two samples or one-way ANOVA test followed by Sidak's post-hoc analysis to test for multiple comparisons. All analyses were performed using GraphPad Prism (Version 9, GraphPad Software, Inc.). A p-value of <0.05 was considered statistically significant. A p-value between 0.05 and 0.1 was considered as a trend towards significance. Values are expressed as mean ± SD.

CHAPTER 3. RESULTS

3.1.1 Cardiac resident Sca-1$^+$ cells and c-kit$^+$ cells demonstrate endothelial cell characteristics

To determine whether cardiac resident Sca-1$^+$ and c-kit$^+$ cells co-expressed endothelial cell marker CD31, single-cell suspension from SD rat hearts was obtained and stained with Sca-1, c-kit, and CD31 antibodies, and flow cytometry analysis was performed. A majority of freshly isolated cardiac resident Sca-1$^+$ cells and c-kit$^+$ cells co-expressed CD31 endothelial cell surface receptor (Figure 4A), demonstrating EC immuno-characteristics. To determine whether these cells exhibited EC functional characteristics, cardiac resident Sca-1$^+$ cells from SD whole hearts were isolated using magnetic sorting and plated on a chamber slide in EGM-2MV 5% CS-FBS overnight, and ability of these cells to uptake Ac-LDL and lectin binding was assessed. Cardiac resident Sca-1$^+$ cells were shown to uptake DiI-AcLDL and bind to lectin-FITC (Figure 4B). Quantification of images showed a majority of Sca-1$^+$ cells took up AcLDL and stained positively for lectin binding, similar to mature endothelial cells (CD31$^+$) isolated from the same rat, after Sca-1$^+$ cells were sorted out (Figure 4C). Overall, these results demonstrate that freshly cardiac resident Sca-1$^+$ cells express cell surface marker for ECs and show functional characteristics of ECs. We also performed Matrigel assay using the freshly isolated cells; however, neither Sca-1$^+$ cells or CD31$^+$ cells formed any noticeable networks.

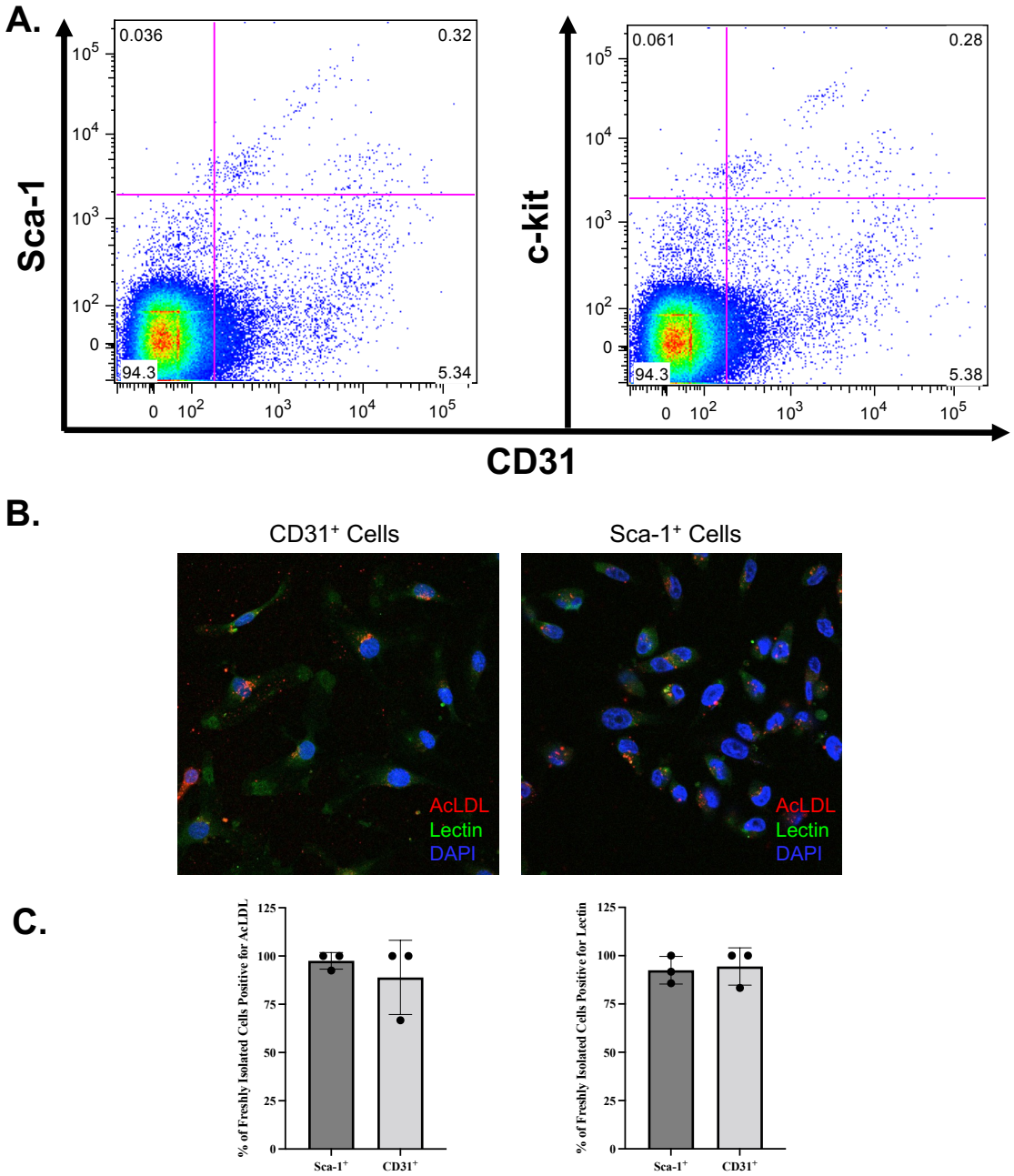

Figure 4. Freshly isolated cardiac resident Sca-1$^+$ cells and c-kit$^+$ cells demonstrate endothelial characteristics. A. Representative flow cytometry images demonstrating Sca-1 and CD31, as well as c-kit and CD31 co-expression from whole heart of SD rats. B. Representative images, and C. quantification of acetylated low-density lipoprotein and lectin-binding assay of cardiac resident Sca-1$^+$ cells isolated from a SD heart through magnetic sorting.

3.1.2 Cultured cardiac resident Sca-1$^+$ cells and CD31$^+$ cells demonstrate endothelial cell characteristics

To determine the morphology of these cells in culture, cardiac resident Sca-1$^+$ isolated from SD hearts through magnetic sorting were plated in a 24-well plate containing EGM-2MV 5% CS-FBS. These cells showed EC cobblestone morphology (Figure 5A). To determine whether these cultured cells exhibit EC characteristics, such as AcLDL uptake, lectin binding, and network formation, cardiac resident Sca-1$^+$ cells from SD whole hearts were isolated using magnetic sorting and cultured using EGM-2MV 5% CS-FBS. Cultured cardiac resident Sca-1$^+$ cells take up AcLDL and bind to lectin-FITC (Figure 5B). Quantification of images showed a majority of Sca-1$^+$ cells isolated had AcLDL uptake and lectin binding, like mature endothelial cells (CD31$^+$) isolated from the same SD rats after Sca-1$^+$ cells were sorted out (Figure 5C). Cardiac resident Sca-1$^+$ cells in culture for 8 weeks, were plated on an angiogenic slide with Matrigel extracellular matrix, and formed networks similar to CD31$^+$ cells isolated from the same SD rat. (Figure 5D). Overall, these data demonstrate that cardiac resident Sca-1$^+$ cells cultured in EGM-2MV 5% CS-FBS express EC cell surface markers and demonstrate EC functional characteristics.

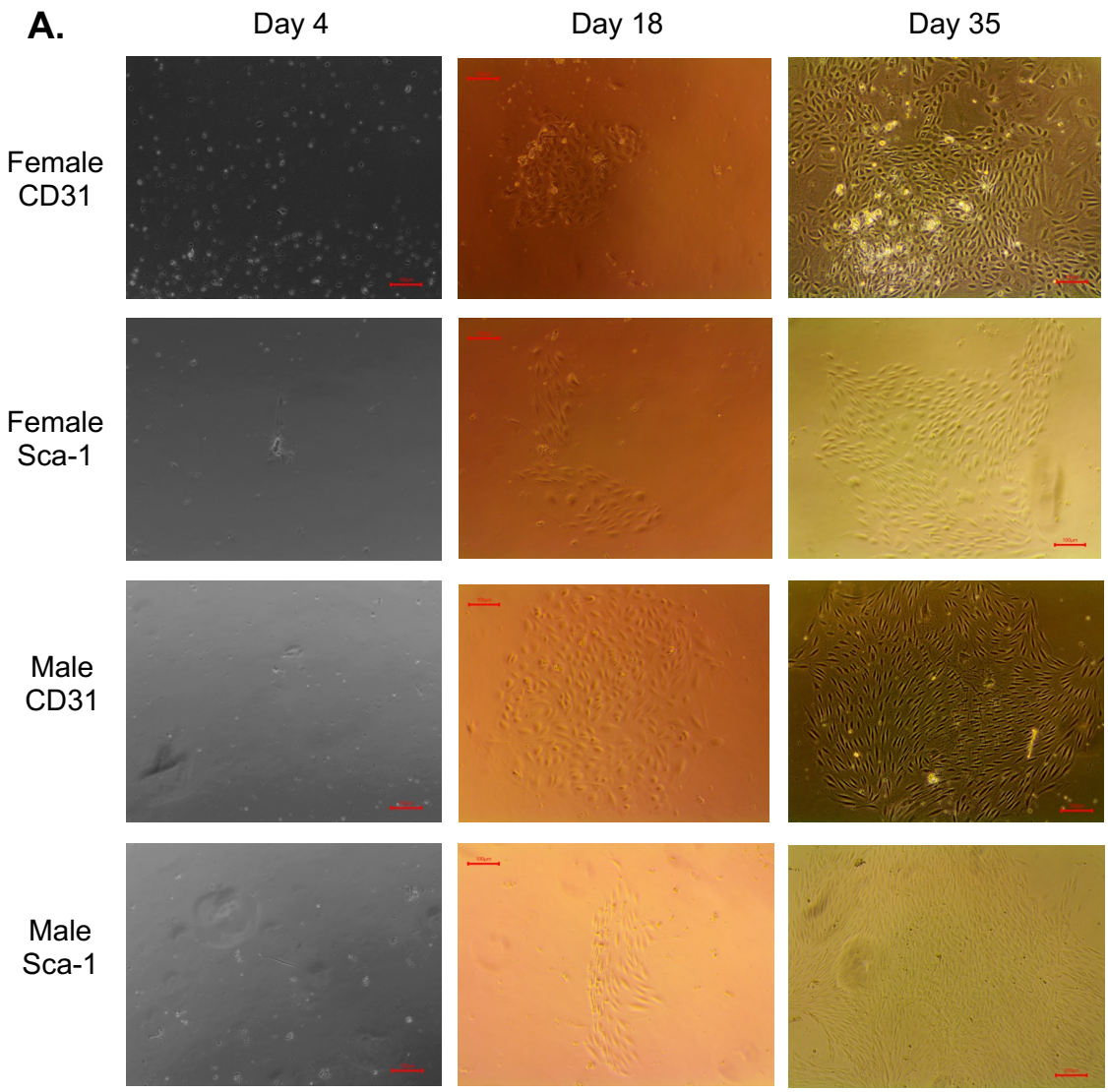
A.
Day 4
Day 18
Day 35
Female CD31
Female Sca-1
Male CD31
Male Sca-1

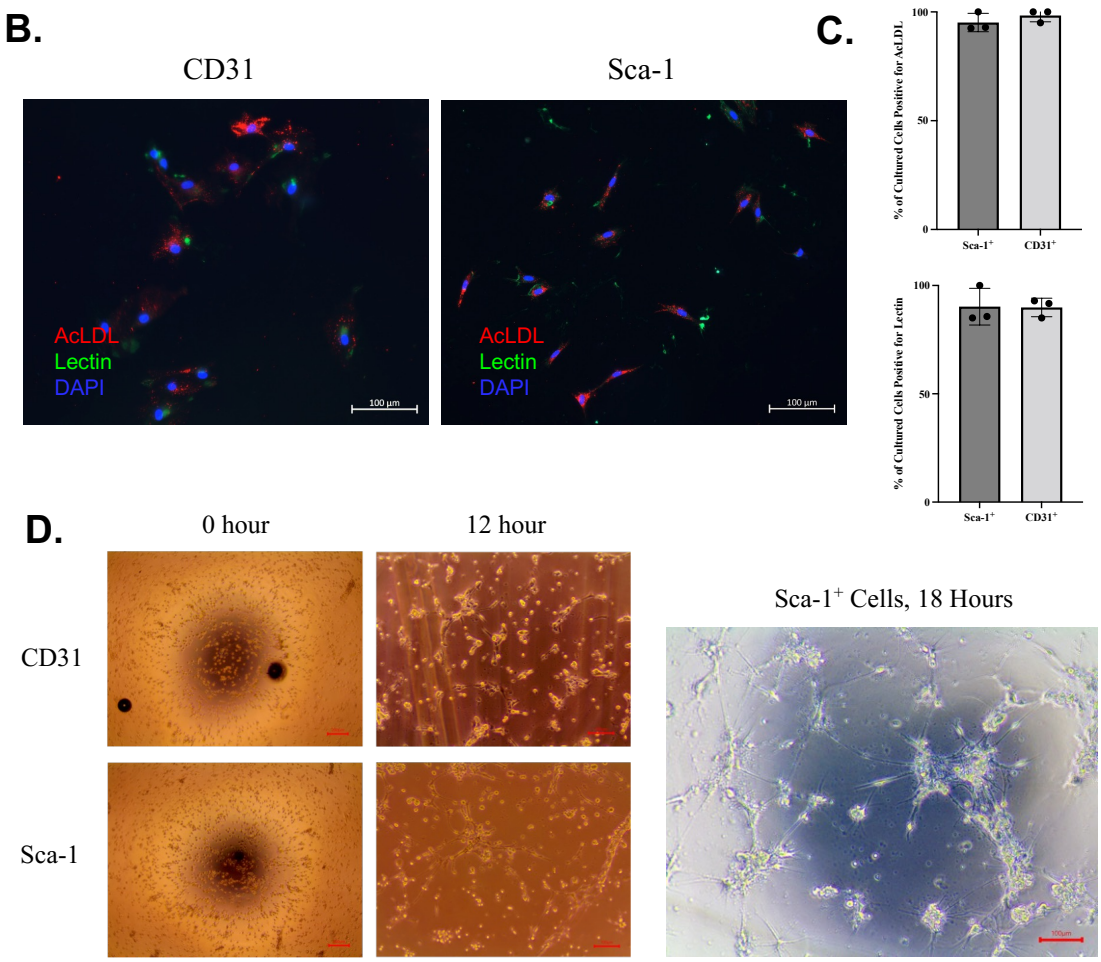

Figure 5. Cultured cardiac resident Sca-1$^+$ cells and CD31$^+$cells demonstrate endothelial cell characteristics. A. Representative images demonstrating endothelial cell cobble-stone morphology of cardiac resident Sca-1$^+$ cells, and CD31$^+$ cells from male and female SD rats isolated from magnetic sorting, cultured in EGM-2MV (phenol free media containing 5% CS-FBS). B. Representative images and C. quantification of acetylated low-density lipoprotein and lectin-binding of cardiac resident Sca-1$^+$ cells isolated from SD heart, n=3. D. Matrigel assay of cultured cardiac resident Sca-1$^+$ cells isolated from SD hearts, after culture for 8 weeks.

3.2 More cardiac resident $CD31^+$, $Sca\text{-}1^+$, $c\text{-}kit^+$, $CD31^+Sca\text{-}1^+$, $CD31^+c\text{-}kit^+$ cells in the RV compared to the LV from flow cytometry analysis

To determine differences in the abundance of these cell populations across the RV and LV, cells isolated from SD rat RV and LV+S were stained with CD31, Sca-1 and c-kit. A higher percentage of $CD31^+$ cells, $Sca\text{-}1^+$ cells, and $c\text{-}kit^+$ cells were observed in the RV compared to the LV of healthy SD rats ($p<0.05$) (Figure 6A-F). Furthermore, a higher percentage of $CD31^+$-$Sca\text{-}1^+$ cells and $CD31^+$-$c\text{-}kit^+$ cells was observed in the RV compared to the LV+S ($p<0.05$) (Figure 6G-J). This data demonstrates a higher abundance of both endothelial and endothelial-like Sca-1 and c-kit expressing cells in the RV compared to the LV+S.

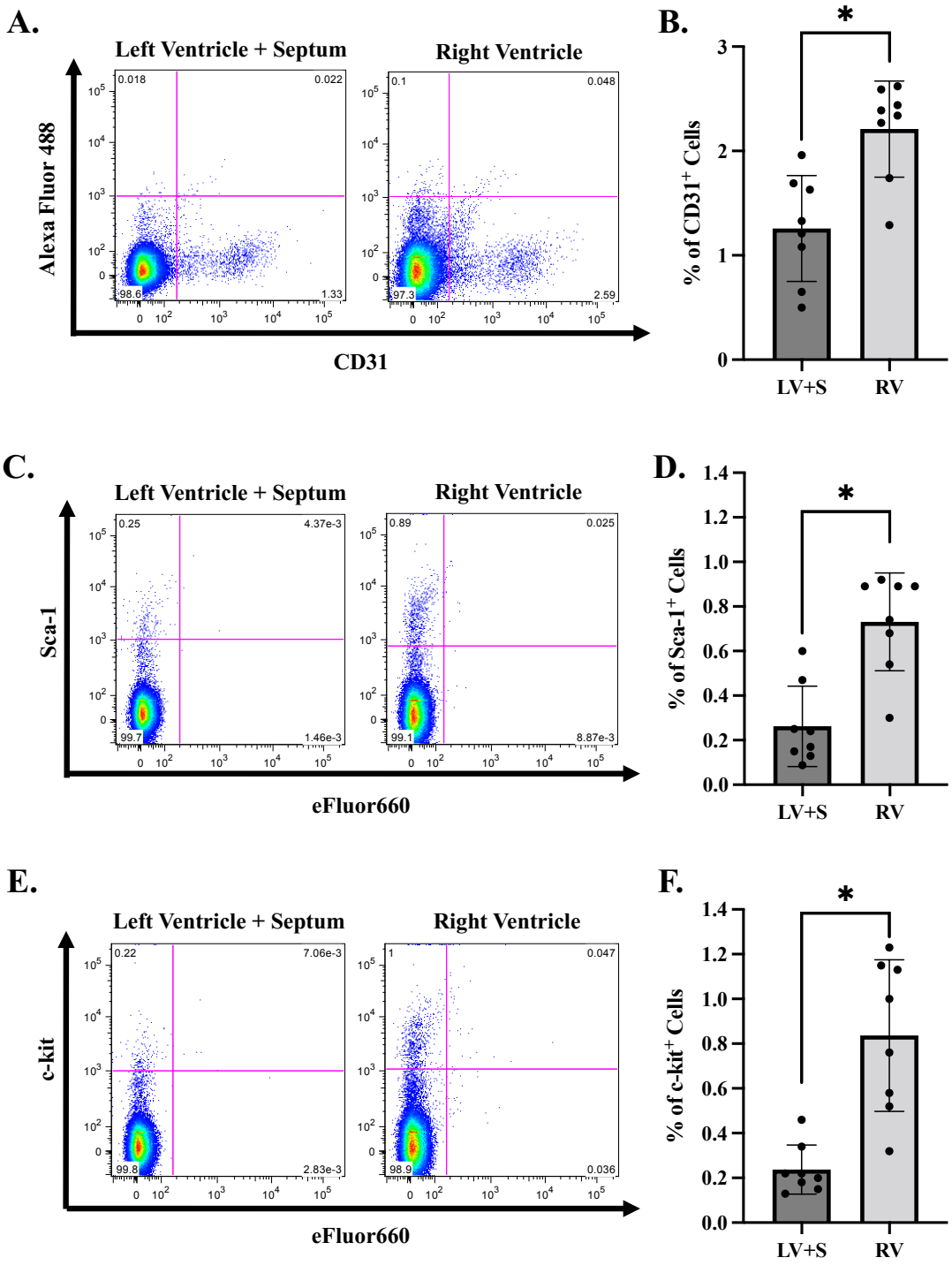
A.
Left Ventricle + Septum
Right Ventricle
Alexa Fluor 488
CD31
0.018
0.022
98.6
1.33
0.1
0.048
97.3
2.59
B.
*
% of CD31+ Cells
LV+S
RV
C.
Left Ventricle + Septum
Right Ventricle
Sca-1
eFluor660
0.25
4.37e-3
99.7
1.46e-3
0.89
0.025
99.1
8.87e-3
D.
*
% of Sca-1+ Cells
LV+S
RV
E.
Left Ventricle + Septum
Right Ventricle
c-kit
eFluor660
0.22
7.06e-3
99.8
2.83e-3
1
0.047
98.9
0.036
F.
*
% of c-kit+ Cells
LV+S
RV

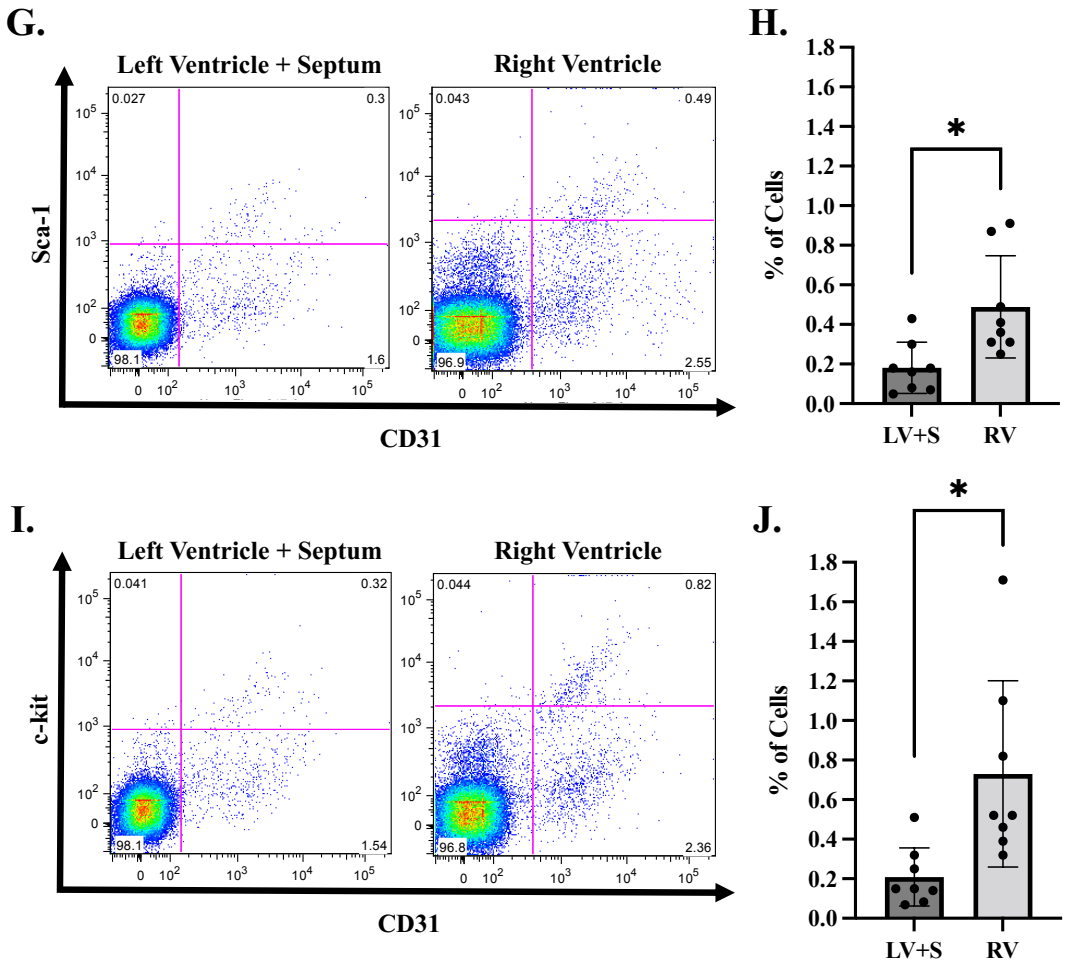

Figure 6. Distribution of cardiac resident CD31$^+$, Sca-1$^+$, c-kit$^+$, CD31$^+$ Sca-1$^+$ cells, and CD31$^+$ c-kit$^+$ cells across the left ventricle + septum, and right ventricle.

A. Representative flow cytometry plots and B. quantification of CD31$^+$ cells. C. Representative flow cytometry plots and D. quantification of Sca-1$^+$ cells. E. Representative flow cytometry plots and F. quantification of c-kit$^+$ cells. G. Representative flow cytometry plots and H. quantification of CD31$^+$Sca-1$^+$ cells. I. Representative flow cytometry plots and J. quantification of CD31$^+$c-kit$^+$ cells. Student t-test used, n=8 biological replicates, *p<0.05 considered significant.

3.3. Abundance of cardiac resident $CD31^+$, $Sca\text{-}1^+$, $c\text{-}kit^+$, $CD31^+Sca\text{-}1^+$, $CD31^+c\text{-}kit^+$ cells were similar in healthy male and female SD rats

To assess abundance of cardiac $Sca\text{-}1^+$ cells and $c\text{-}kit^+$ cells in healthy male and female rats, cells isolated from the RV and LV+S of SD rats (9-14 week old) were stained with CD31, Sca-1, and c-kit. There was no age difference between male and female rats; however female rats had significantly lower body weights compared to male rats (Figure 7). Consistent with body weights, male rats had a trend toward significantly higher RV and LV+S weights compared to females (Figure 7). Importantly, no significant difference in FI of male and female rats was observed (Figure 7). Flow cytometry analysis of the cells isolated from healthy SD rat RV and LV+S demonstrated no significant differences in $CD31^+$ cells, $Sca\text{-}1^+$ cells, and $c\text{-}kit^+$ cells (Figure 8A-F). Furthermore, we observed similar abundance of $CD31^+Sca\text{-}1^+$ cells and $CD31^+c\text{-}kit^+$ cells in healthy male and female SD rats (Figure 8G-J).

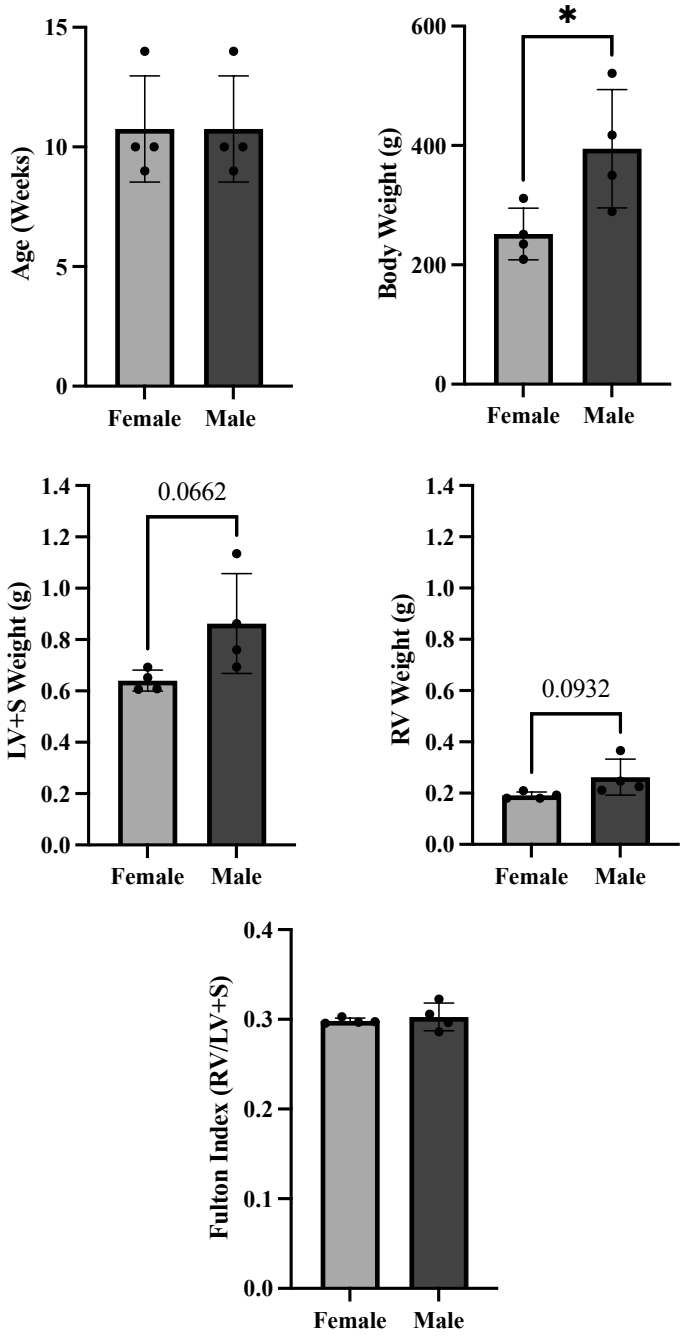

Figure 7. Characteristics of SD rats used for flow cytometry experiments. Age (in weeks), body weight (grams), LV+S weight (grams), RV weight (grams), and FI (RV/LV+S) of SD rats. Student t-test used, n=4 biological replicates, *p<0.05 considered significant.

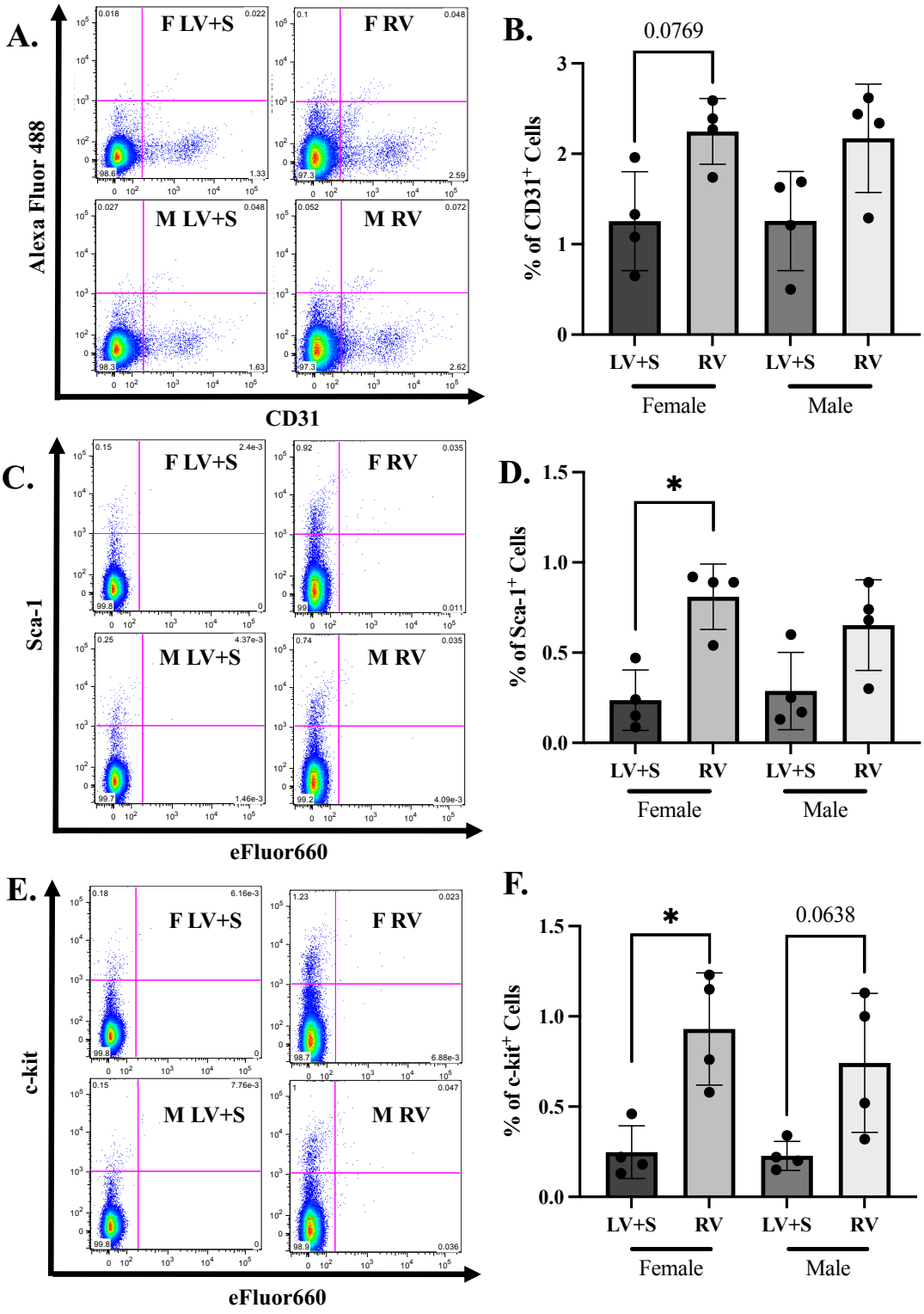
A.
F LV+S
F RV
M LV+S
M RV
Alexa Fluor 488
CD31
B.
0.0769
% of CD31+ Cells
LV+S
RV
LV+S
RV
Female
Male
C.
F LV+S
F RV
M LV+S
M RV
Sca-1
eFluor660
D.
*
% of Sca-1+ Cells
LV+S
RV
LV+S
RV
Female
Male
E.
F LV+S
F RV
M LV+S
M RV
c-kit
eFluor660
F.
*
0.0638
% of c-kit+ Cells
LV+S
RV
LV+S
RV
Female
Male

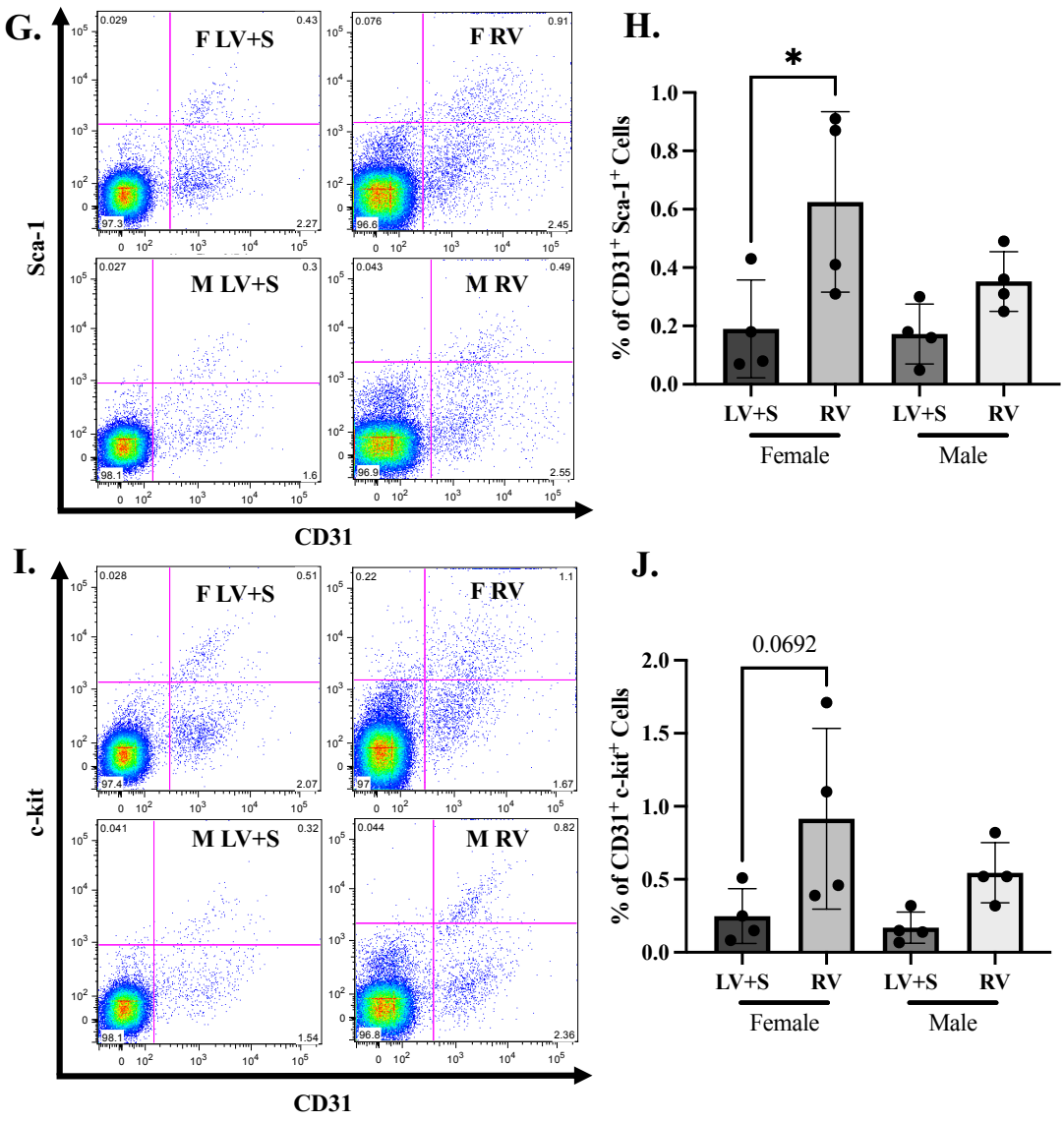

Figure 8. Percentage of cardiac resident CD31$^+$ cells, Sca-1$^+$ cells, c-kit$^+$ cells, CD31$^+$Sca-1$^+$ cells, and CD31$^+$ c-kit$^+$ cells in the right ventricle and left ventricle + septum, from SD rats. A. Representative flow cytometry plots and B. quantification of CD31$^+$ cells. C. Representative flow cytometry plots and D. quantification of Sca-1$^+$ cells. E. Representative flow cytometry plots and F. quantification of c-kit$^+$ cells. G. Representative flow cytometry plots and H. quantification of CD31$^+$Sca-1$^+$ cells. I. Representative flow cytometry plots and J. quantification of CD31$^+$c-kit$^+$ cells. Two-way ANOVA with Sidak's post-hoc analysis used, n=4 biological replicates per tissue type, *p<0.05 considered significant.

3.4 Strain difference in abundance of cardiac resident $CD31^+$, $Sca\text{-}1^+$, $c\text{-}kit^+$, $CD31^+Sca\text{-}1^+$, $CD31^+c\text{-}kit^+$ cells

To determine whether strain differences exist in the abundance of $CD31^+$, $Sca\text{-}1^+$, $c\text{-}kit^+$, $CD31^+Sca\text{-}1^+$, $CD31^+c\text{-}kit^+$ cells, we compared the abundance of these cells between Fischer CDF rats and SD rats. It is important to note that Fischer CDF rats are more susceptible to the development of RHF in response to elevated RV afterload compared to better RV adaptation and survival in SD rats. Considering the role of RV angiogenesis in adaptation to elevated RV afterload and the endothelial progenitor nature of cardiac $Sca\text{-}1^+$ cells and $c\text{-}kit^+$ cells, we compared the abundance of these cells in RV and LV+S of SD and Fischer CDF rats. No statistical differences were seen in the age of SD compared to Fischer CDF rats (Figure 9). SD rats had higher body weight as well as higher LV+S and RV weight compared to Fischer CDF rats (Figure 9). No significant difference in FI of SD and Fischer CDF rats was observed (Figure 9). Single stained samples showed more $CD31^+$ cells in the RV and LV+S of Fischer rats compared to SD rats (Figure 10A-B). Furthermore, more $Sca\text{-}1^+$ cells and $c\text{-}kit^+$ cells were observed in the LV+S of Fischer CDF rats compared to SD rats (Figure 10C-F); however, no difference was observed in the abundance of these cells between the RV of SD and Fischer CDF rats. Similarly, a trend towards more $CD31^+Sca\text{-}1^+$ cells (Figure 10G-H) and higher $CD31^+c\text{-}kit^+$ cells abundance was observed in LV+S of Fischer CDF rat compared to SD rats ($p<0.05$) (Figure 10I-J). No differences were observed in $CD31^+Sca\text{-}1^+$ cells (Figure 10G-H) and $CD31^+c\text{-}kit^+$ cells in the RV of SD and Fischer CDF rats.

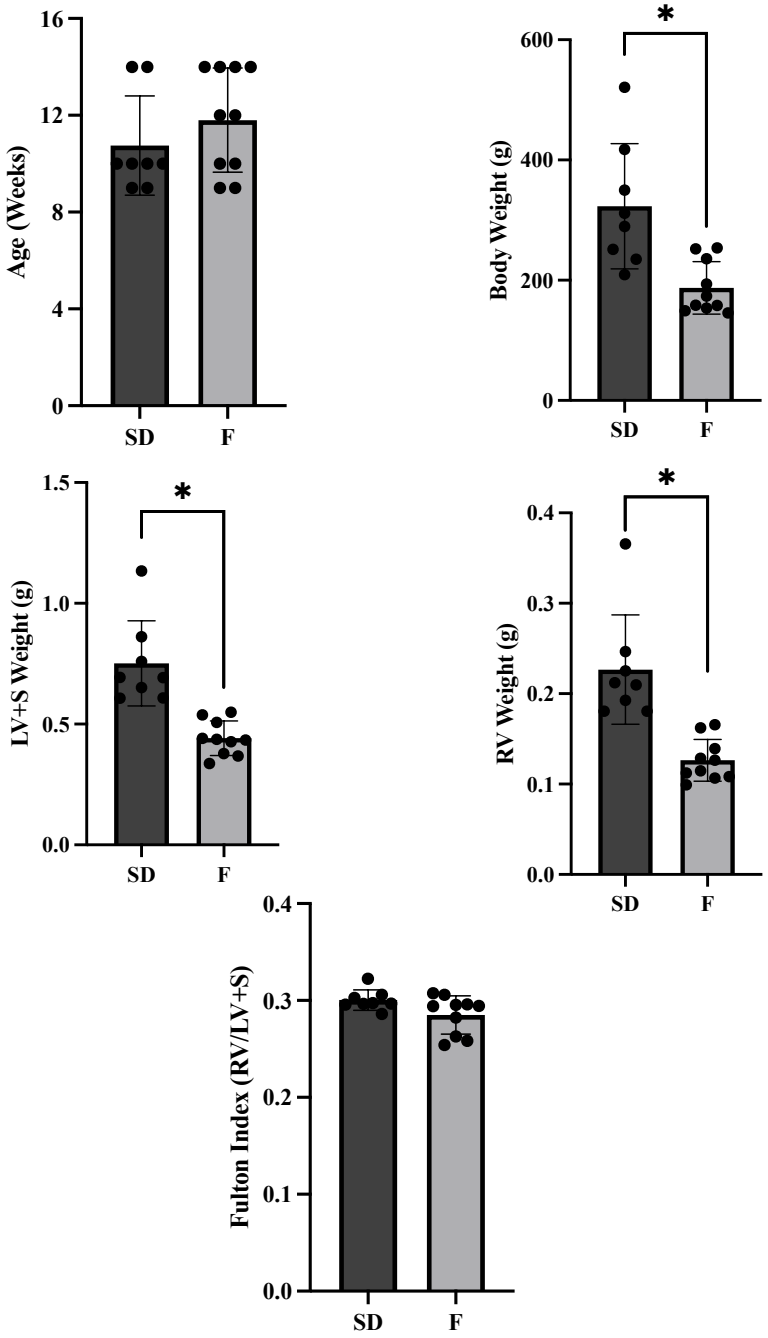

Figure 9. Characteristics of SD and Fischer CDF rats used for flow cytometry experiments. Age (in weeks), body weight (grams), LV+S weight (grams), RV weight (grams), and FI (RV/LV+S) of SD and Fischer CDF (F) rats. Student t-test used, n=8-10 biological replicates per rat strain, *$p<0.05$ considered significant.

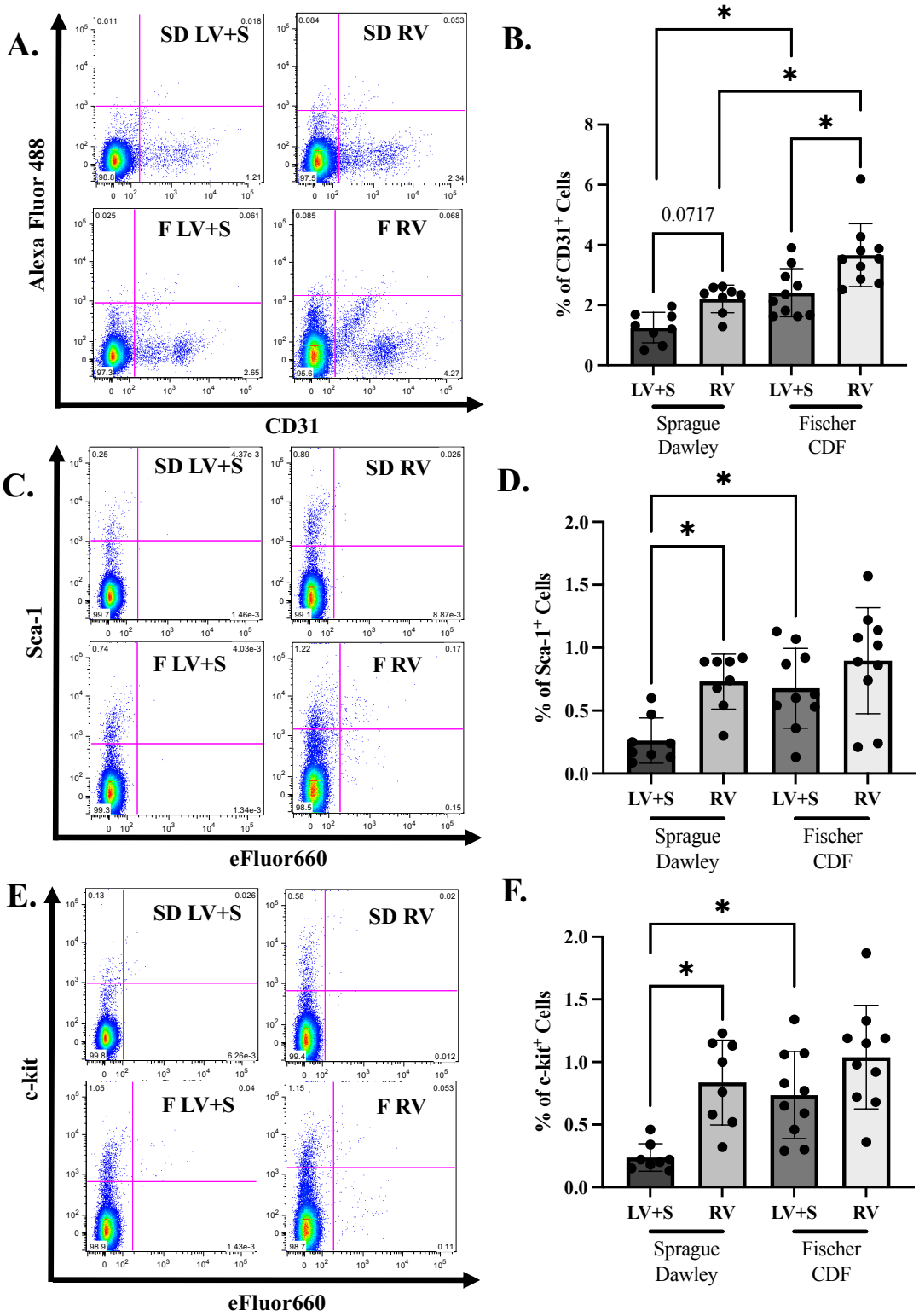
A.
SD LV+S
SD RV
F LV+S
F RV
Alexa Fluor 488
CD31
B.
% of CD31+ Cells
0.0717
LV+S
RV
LV+S
RV
Sprague Dawley
Fischer CDF
C.
Sca-1
eFluor660
D.
% of Sca-1+ Cells
E.
c-kit
eFluor660
F.
% of c-kit+ Cells

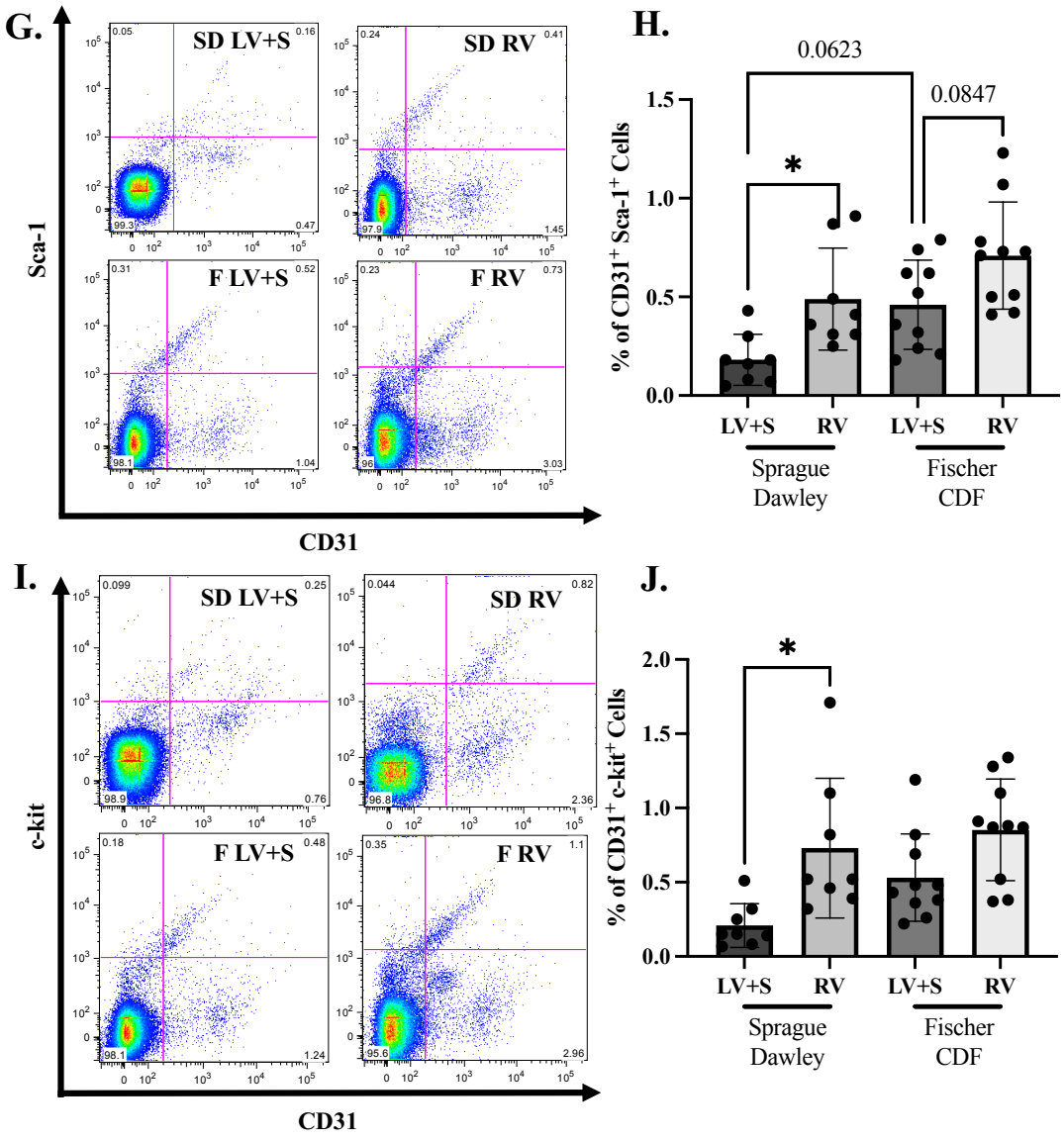

Figure 10. No major strain differences in number of cardiac resident CD31$^+$, Sca-1$^+$, and c-kit$^+$, CD31$^+$Sca-1$^+$ and CD31$^+$c-kit$^+$ cells. A. Representative flow cytometry plots and B. quantification of cardiac CD31$^+$ cells from SD and Fischer CDF rats. C. Representative flow cytometry plots and D. quantification of cardiac Sca-1$^+$ cells SD and Fischer CDF rats. E. Representative flow cytometry plots and F. quantification of cardiac c-kit$^+$ cells SD and Fischer CDF rats. G. Representative flow cytometry plots and H. quantification of cardiac CD31$^+$Sca-1$^+$ cells from SD and Fischer CDF rats. I. Representative flow cytometry plots and J. quantification of cardiac CD31$^+$c-kit$^+$ cells SD and Fischer CDF rats. Two-way ANOVA with Sidak's post-hoc analysis used, n=8-10 biological replicates per rat strain, *p<0.05 considered significant.

3.5 Marked reduction in abundance of cardiac CD31$^+$, Sca-1$^+$, c-kit$^+$, CD31$^+$Sca-1$^+$ and CD31$^+$c-kit$^+$ cells in the RV of rats subjected to MCT model of severe PH and RHF

To determine whether pathological RV remodeling influenced the abundance of these cells, 10-week-old male and female Fischer CDF rats were injected with MCT and the abundance of CD31$^+$, Sca-1$^+$, c-kit$^+$, CD31$^+$Sca-1$^+$, and CD31$^+$c-kit$^+$ cells in the RV was assessed at 4 weeks post MCT injection. Both the male and female Fischer CDF rats injected with MCT were older than naïve controls ($p<0.05$) (Figure 11A); however, no significant difference in body weights or LV+S weights were observed between naïve and MCT treated rats (Figure 11B-C). Importantly, male but not female MCT rats had greater RV weights compared to respective naïve controls (Figure 11D). FI was significantly elevated in MCT-treated male and female rats compared to naïve controls (Figure 11E). RVSP was elevated in response to MCT treatment (Male: ~40mmHg, Female ~39mmHg). Compared to naïve controls, marked reduction in CD31$^+$ cells, Sca-1$^+$ cells, and c-kit$^+$ cells was observed in the RV of both the male and female MCT-treated rats (Figure 12A-F). Similarly, we observed significant decrease in CD31$^+$Sca-1$^+$ cells and CD31$^+$c-kit$^+$ cells in MCT-treated male and female rat RVs compared to naïve controls (Figure 12G-J). With the limited sample-size of the current study, we did not observe significant differences in abundance of CD31$^+$ cells (Figure 12B), Sca-1$^+$ cells (Figure 12D), c-kit$^+$ cells (Figure 12F), CD31$^+$Sca-1$^+$ cells (Figure 12H) and CD31$^+$c-kit$^+$ cells (Figure 12J) between the RVs of male and female rats.

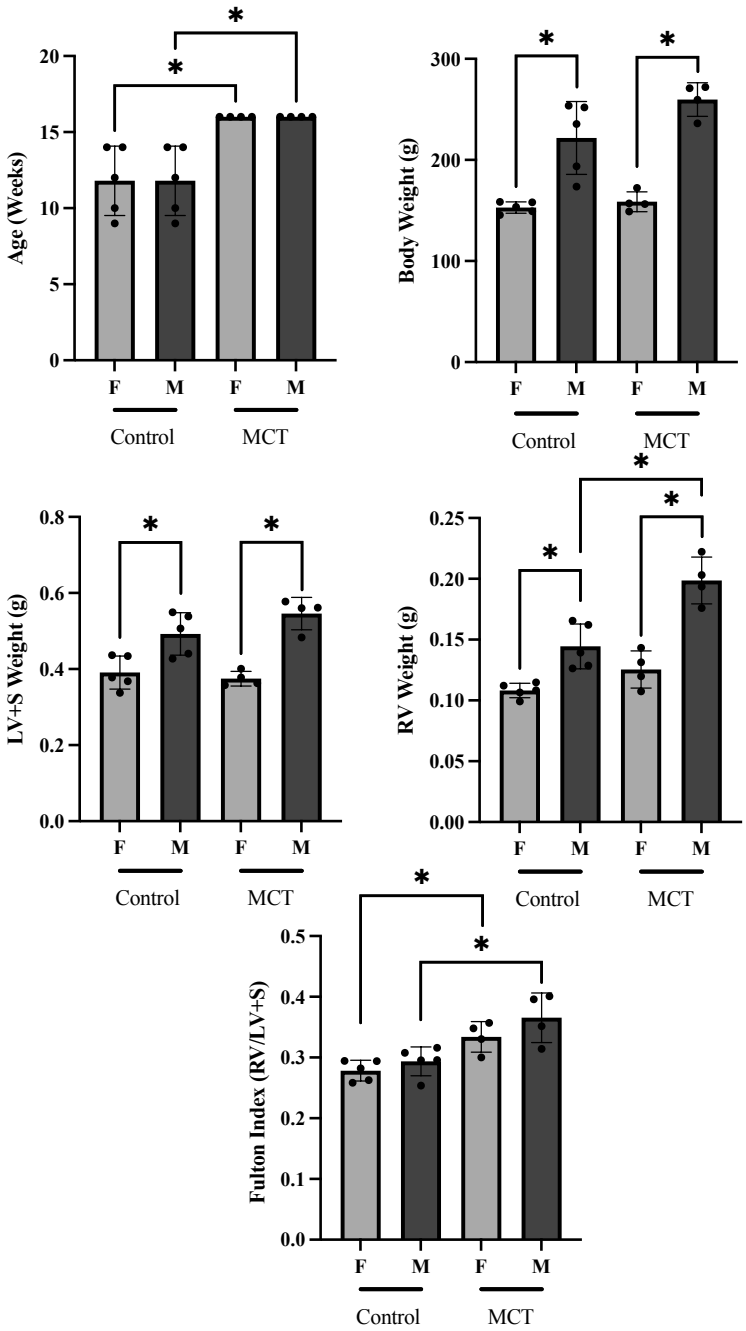

Figure 11. Characteristics of monocrotaline-injected Fischer CDF rats used for flow cytometry experiments. Age (in weeks), body weight (grams), LV+S weight (grams), RV weight (grams), and FI (RV/LV+S) of Fischer CDF naïve controls compared to MCT injected Fischer CDF rats, and right ventricular systolic pressure of two male and two female MCT injected Fischer CDF rats. Two-way ANOVA with Sidak's post-hoc analysis used, n=4-5 biological replicates per condition, *p<0.05 considered significant to experimental condition control, #p<0.05 considered significant to sex-matched control.

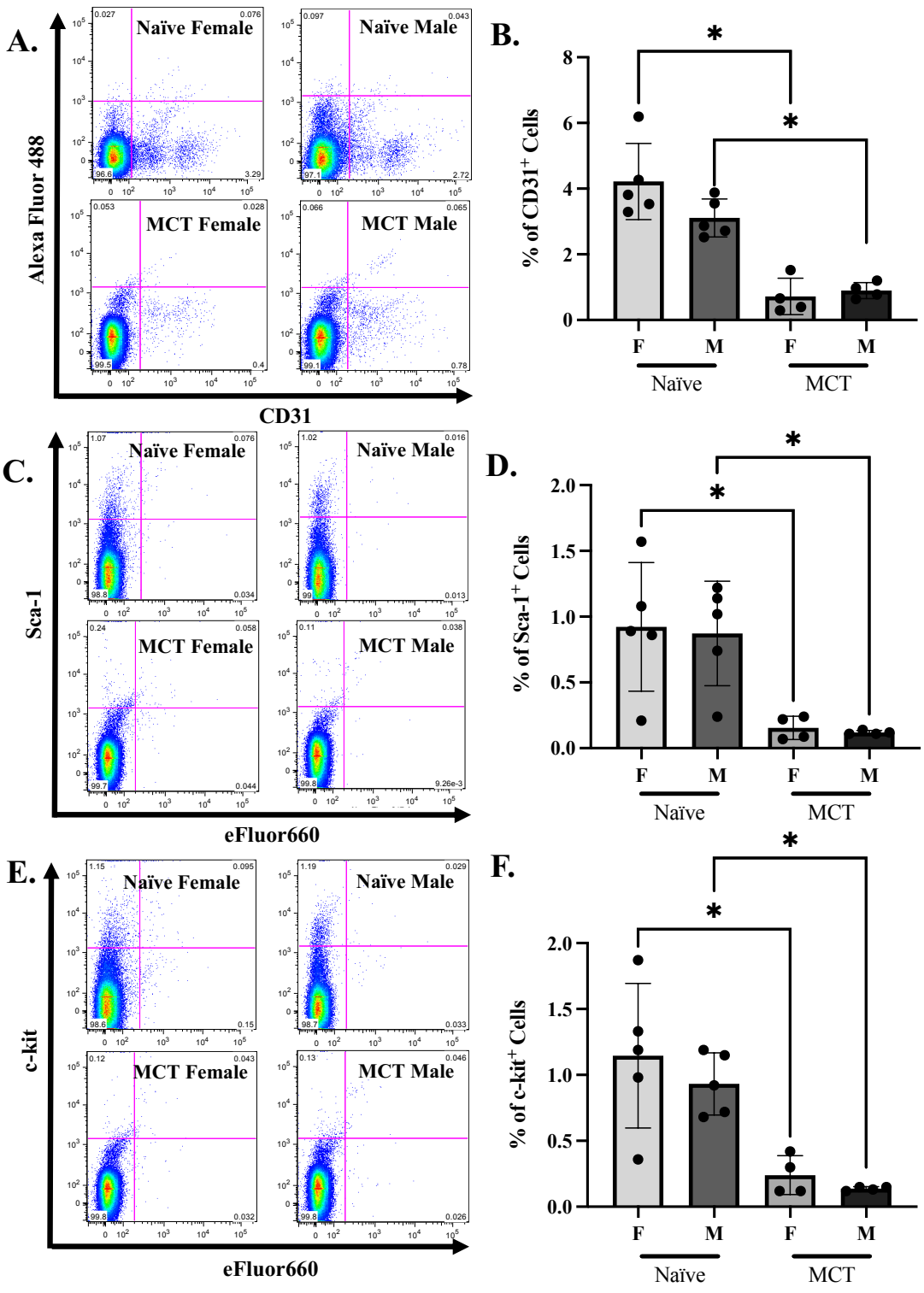
A.
Naïve Female
Naïve Male
MCT Female
MCT Male
Alexa Fluor 488
CD31
B.
% of CD31+ Cells
F
M
F
M
Naïve
MCT
C.
Naïve Female
Naïve Male
MCT Female
MCT Male
Sca-1
eFluor660
D.
% of Sca-1+ Cells
F
M
F
M
Naïve
MCT
E.
Naïve Female
Naïve Male
MCT Female
MCT Male
c-kit
eFluor660
F.
% of c-kit+ Cells
F
M
F
M
Naïve
MCT

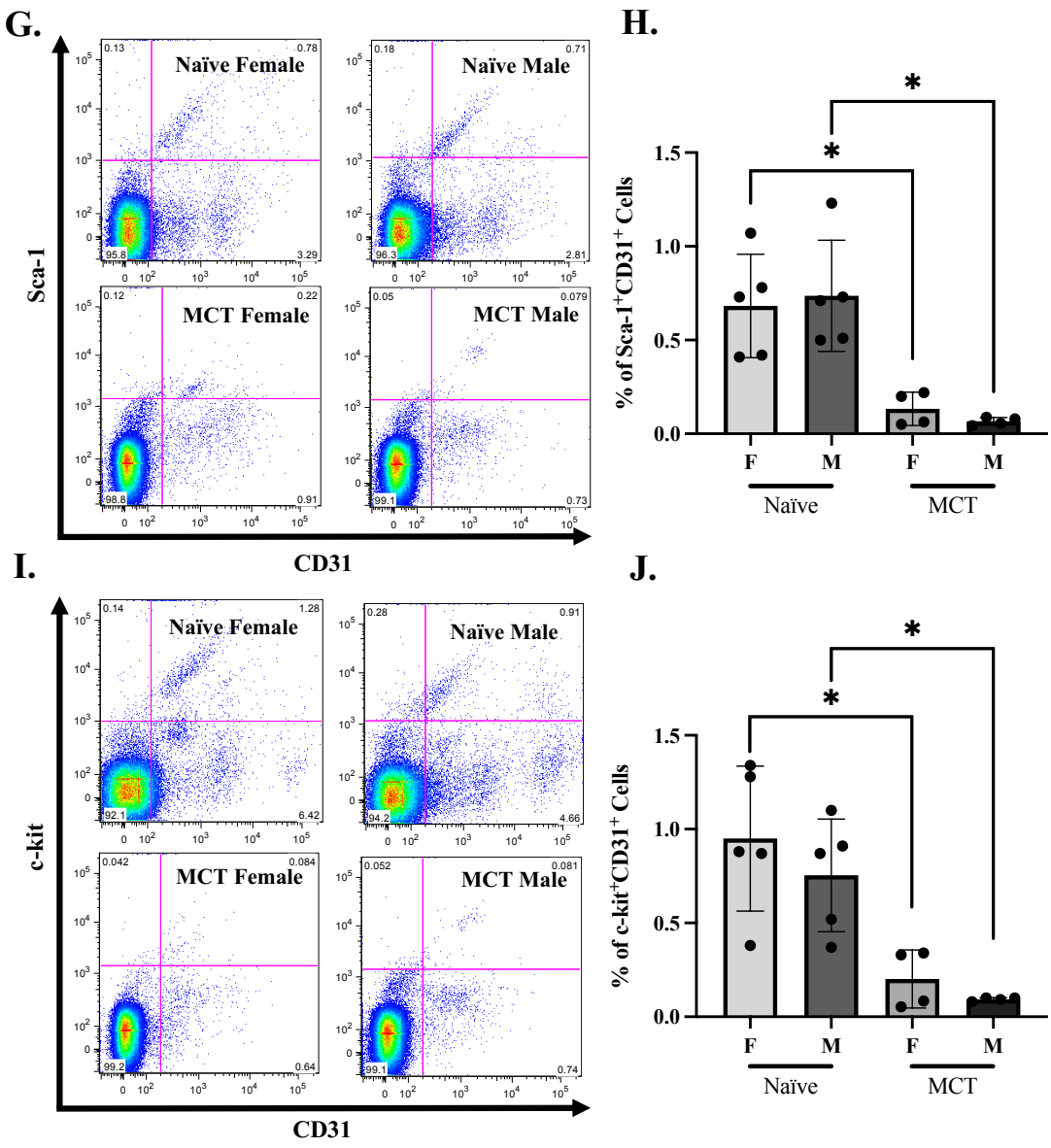

Figure 12. MCT Reduces the Percentage of Cardiac CD31$^+$, Sca-1$^+$, and c-kit$^+$, CD31$^+$Sca-1$^+$ and CD31$^+$c-kit$^+$ cells in the right ventricle. A. Representative flow cytometry plots and B. quantification of cardiac CD31$^+$ cells, C. Representative flow cytometry plots and D. quantification of cardiac Sca-1$^+$ cells, E. Representative flow cytometry plots and F. quantification of cardiac c-kit$^+$ cells, G. Representative flow cytometry plots and H. quantification of cardiac CD31$^+$ Sca-1$^+$ cells, and I. Representative flow cytometry plots and J. quantification of cardiac CD31$^+$ c-kit$^+$ cells, from naïve and monocrotaline injected Fischer rat right ventricles. Two-way ANOVA with Sidak's post-hoc analysis used, n=4-5 biological replicates per condition, *p<0.05 considered significant.

CHAPTER 4. DISCUSSION

4.1 General Discussion

Our data demonstrate endothelial cell characteristics of cardiac resident Sca-1$^+$ cells and c-kit$^+$ cells. We assessed differences in abundance of these cells in both the ventricles of the heart and demonstrated higher abundance of Sca-1$^+$ cells and c-kit$^+$ cells in the RV of the heart compared to the LV+S. In addition, we examined differences in abundance of cardiac Sca-1$^+$ cells and c-kit$^+$ cells between SD (RHF resistant) and Fischer CDF (RHF susceptible) rats, as well as assessed abundance of these cells in male and female rats. While we observed some differences in abundance of these cells in the LV+S between strains, we did not observe any significant differences in these cells in the RV of healthy rats. Similarly, no major impact of biological sex was observed on abundance of Sca-1$^+$ cells and c-kit$^+$ cells in healthy rats. Finally, we demonstrated marked reduction in Sca-1$^+$ cells and c-kit$^+$ cells in the RV of rats subjected to MCT injection.

Previous studies have characterized Sca-1$^+$ cells and c-kit$^+$ cells as expressing endothelial markers such as Tie2, and CD31/PECAM by immunofluorescence in representative mouse heart sections[27,28]. Those studies also confirmed that cardiac resident Sca-1$^+$ cells and c-kit$^+$ cells did not co-express cardiac troponin T or Nkx2.5 and contributed minimally to the development of new cardiomyocytes[27,28,29,30]. While these studies suggest an endothelial nature of cardiac Sca-1$^+$ cells and c-kit$^+$ cells, the findings were limited to immuno-characterization of 5μm sections, whereas whole organ immuno-characterization and *in vitro* functional assessment was not performed. Studies performed in our lab addressed these limitations using an approach for immuno and functional characterization of these cells in a rat model. Similar to mature EC isolated from the heart (in this study) and EPC obtained from bone-marrow[120], most of the freshly isolated cardiac

Sca-1$^+$ cells and c-kit$^+$ cells express cell surface markers of endothelial cells, uptake Ac-LDL, and demonstrate lectin binding. We were unable to determine the network-forming ability of freshly isolated cardiac resident Sca-1$^+$ cells. However, it is important to note that CD31$^+$ cells plated on Matrigel extracellular matrix immediately after isolation also did not form networks. Therefore, we believe either our harvesting procedure inhibited the network-forming ability of both the cardiac resident Sca-1$^+$ cells and CD31$^+$ cells or the number of viable cells after the isolation were insufficient to form networks when plated on Matrigel extracellular matrix. However, when cultured in endothelial growth media, these cells showed cobblestone morphology and formed networks on Matrigel that were similar to mature EC from the heart and EPC obtained from bone-marrow[120]. Together, consistent with previous reports[27,28,29,30], our data showed that the vast majority of the cardiac Sca-1$^+$ cells and c-kit$^+$ cells are endothelial in nature and may be tissue-resident endothelial progenitor-like cells.

Importantly, our data also demonstrate there are more of these cardiac Sca-1$^+$ cells and c-kit$^+$ cells in the RV compared to the LV+S. This finding emphasizes the importance of conducting research with the RV as an independent variable, as there are key physiologically differences compared to the LV, and RV function is highly associated with survival outcomes in many cardiac-related diseases, such as PH, HFpEF, and more[92,121,122]. In physiological conditions, the RV is more vascularized than the LV[119], which matches our flow cytometry data, showing more CD31$^+$ cells in the RV compared to the LV+S. Considering the cardiac Sca-1$^+$ cells and c-kit$^+$ cells are endothelial progenitor-like cells, a higher abundance of these cells in the RV may have physiological relevance and these cells may be involved during RV vascular remodeling.

Current literature cites more circulating EPCs associated with the female sex[71]. Furthermore, more cardiac resident c-kit$^+$ cells are seen in females[72]. Additionally, the female sex hormone estradiol was shown to increase proliferation and decrease senescence of these cells[75,76]. Therefore, sex differences in cardiac Sca-1$^+$ cells and c-kit$^+$ cells were expected; however, we did not witness any sex differences in the abundance of these cells. These differences could arise from different types of cells (circulating EPCs versus cardiac Sca-1$^+$ cells and c-kit$^+$ cells) or differences in the method of assessment. The previous study assessed the number of c-kit$^+$ cells from cultured cells from human heart compared to our assessment of the percentage of c-kit$^+$ cells and Sca-1$^+$ cells in freshly isolated cells.

Previous research has demonstrated that Fischer rats develop maladaptive RV remodeling and are susceptible to development of RHF in the SUHx model, whereas SD rats show adaptive remodeling and are protected against RHF[103]. In that study, the maladaptive RV remodeling and RHF were associated with a lack of an angiogenic response in male Fischer CDF rats compared to the adequate angiogenic response in SD rats. Considering the EPC-like nature of Sca-1$^+$ cells and c-kit$^+$ cells and the higher RV abundance of these cells, we hypothesized that Fischer rats may contain less of these cells compared to SD rats. Contrary to our hypothesis, we noted higher abundance of CD31$^+$ cells, Sca-1$^+$ cells, and c-kit$^+$ cells in Fischer CDF rats compared to SD. This could be due to the differences in sub-strains of SD rats. Previous studies have reported important differences in various parameters between SD rats from two different suppliers, Harlan Laboratories and Charles River Labs. Another article comparing SD rats from Charles River and Harlan laboratories found that Charles River SD rats are susceptible to vascular diseases, and respond to SU5416 and develop severe PH in the absence of hypoxia, a

response that was absent from Harlan SD rats[98]. Similar to Fischer CDF rats, Charles River SD rats showed poor RV adaptation compared to Harlan SD rats in the SUHx model[98]. These observations may explain the lack of differences in the abundance of Sca-1$^+$ cells and c-kit$^+$ cells between Charles River SD rats and Fischer CDF rats in our studies. To assess differences in abundance of Sca-1$^+$ cells and c-kit$^+$ cells between adaptive and mal-adaptive models of RV remodeling, Fischer CDF rats should be compared to Harlan SD rats.

Recent studies have demonstrated that adverse RV remodeling and RHF is associated with poor RV angiogenic response during RV adaptation to increased afterload[103,105,124]. For instance, reduced vascular density has been reported in patients with RHF, and it is suggested to be one of the major differentiating events between adaptive and mal-adaptive RV remodeling[105]. Similarly, preclinical studies have demonstrated that adaptive RV remodeling is accompanied by angiogenesis, whereas mal-adaptive remodeling is associated with an inadequate angiogenic response[103]. This study demonstrated reduction in RV vascular density during RV remodeling with a greater reduction in Fischer CDF rats. In our study, we observed a marked reduction in the abundance of CD31$^+$, Sca-1$^+$, c-kit$^+$, CD31$^+$Sca-1$^+$, and CD31$^+$c-kit$^+$ cells that was consistent with a reduction vascular density during RV remodeling in Fischer CDF rats. It is also possible that the reduction in these cell populations was due to a direct effect of MCT-P. After injection, monocrotaline is metabolized to monocrotaline pyrrole in the liver by cytochrome P-450[93]. The drug was shown to have damage in pulmonary vasculature just hours after injection[125]. The drug is known to target endothelial cells of pulmonary vasculature; however, other organs may show signs of damage as well. Therefore, further

investigation using another model of RV overload would be important to understand the relative impact of RV pathology compared to effect of MCT on the abundance of these cell populations. Importantly, we qualitatively noted an increase in variance in the female MCT group. One study points towards the effect of sex hormones on the function of Sca-1^{+} cells in pathological conditions such as myocardial ischemia[77]. Another study was able to show estradiol increasing the levels of circulating EPCs in ovariectomized estradiol treated mice, after induction of an MI[78]. Therefore, sex differences in the abundance of these cells in pathological conditions may be observed. However, currently, we did not observe sex differences in the abundance of these cells under MCT induced pathological RV remodeling. Further investigation is warranted to determine whether sex differences exist in the abundance of this cell population in other models of RHF.

4.2 Other Considerations and Limitations

The antibodies available for rats limited our study. Through antibody optimization, we were able to determine the efficacy of Sca-1 from Millipore, and c-kit from MyBioSource. However, both antibodies were raised in rabbits, and would require more optimization before being used in the same sample. At this point we are currently unable to analyze and interpret the co-expression of c-kit and Sca-1. Zhang, et al. in 2019 were able to quantify that ~51.8% of Sca-1 expressing cells co-expressed c-kit in a 4-month-old mouse heart[28]. It would be interesting to determine the relationship that Sca-1 expressing cells share with c-kit expressing cells in rats. We are currently exploring options to allow for the co-staining of both Sca-1 and c-kit, either by using different hosts, or using a primary-conjugated antibody.

We are also limited by the use of EGM-2MV + 5% CS-FBS with our culture of cardiac resident Sca-1$^+$ cells. This media contains growth factors designed for the culture of endothelial cells. Instead, stem cell media may be used to ensure the media does not induce the differentiation of these cells towards a specific lineage.

Another limitation of our study is the use of the MCT model. MCT is a drug that causes endothelial cell apoptosis. MCT is metabolized to MCT-P in the liver, and the model primarily causes apoptosis of endothelial cells in the pulmonary artery due to its close proximity to the liver[126]. This causes an increase in afterload of the RV, which in turn causes pathological remodeling. Through our flow cytometry analyses, we noted a decrease in the number of CD31$^+$ cells in the RV, 4 weeks after MCT injection. Therefore, it is possible that the toxin exhibited its effects on cardiac resident endothelial and endothelial-like Sca-1 and c-kit expressing cells. To mitigate this, we aimed to use the Sugen hypoxia and PAB models of RV remodeling, however we are currently not equipped to perform these experiments to look at the abundance of this population through our global approach of digesting the heart and staining for flow cytometry analysis.

4.3 Future Directions

As the objective of these experiments was exploratory, there are many future directions for this project. Firstly, we would like to look at the proliferative capacity of Sca-1$^+$ cells compared to CD31$^+$ cells isolated from the same animal. Using cells isolated from the same animal, we can determine the passage limit of both cell populations, to understand cell senescence limits. Furthermore, it would be interesting to look at the network forming ability of these cells *in vivo.* A matrigel plugin assay can be used to determine angiogenic potential. Matrigel, as well as these cardiac resident Sca-1$^+$ and c-

kit$^+$ cells can be injected and left before their excision and analysis of network formation[127]. EPCs are loosely defined by "an endothelial cell phenotype, significant proliferative potential, and the capacity to self-assemble into functional blood vessels *in vivo*"[68]. We have characterized these cells as having an endothelial cell phenotype by CD31 expression, cobblestone morphology, AcLDL uptake, lectin binding, and network formation *in vitro*. Therefore, by determining the proliferative capacity and *in vivo* angiogenic potential of these cells, it can be further understood whether these cells can be characterized as CEPCs.

Furthermore, we wish to conduct functional characterization of cardiac resident c-kit$^+$ cells. From initial trial runs, it was clear that more optimization was needed for the isolation of cardiac resident c-kit$^+$ cells. Due to time constraints, we chose to isolate and functionally characterize cardiac resident Sca-1$^+$ cells. We are currently looking to isolate cardiac resident c-kit$^+$ cells to perform AcLDL uptake, lectin binding assays, matrigel assays, as well as to determine the morphology of these cells. This will allow us to further characterize cardiac resident c-kit$^+$ cells as endothelial in nature.

We also wish to use markers of other cardiac resident cells that would be relevant to further understand the identity of these cells. Markers such as α-SMA for smooth muscle cells, or cardiac troponin T for cardiomyocytes, could be used in conjunction with Sca-1 and c-kit to determine if these cells can be attributed to another lineage. Using a global approach of digesting the entire heart, staining, and analyzing through flow cytometry is an efficient way to assess the expression of cell surface receptors of these cells most similarly to *in vivo* conditions. Therefore, the nature of cardiac resident Sca-1$^+$ and c-kit$^+$ cells can be further elucidated using other cell surface receptor antibodies.

Through the use of other antibodies, we may also be able to better immuno-characterize these cells. Initially, we sought to create a panel of antibodies that could be used for these studies. CD200 (commonly expressed on B cells, dendritic cells, activated T cells, and vascular endothelial cells), CD146 (commonly expressed on vascular endothelial cells, smooth muscle cells, and pericytes), as well as CD133 (commonly expressed on EPCs, hematopoietic stem cells, fetal brainstem cells, and prostate epithelial cells) were all considered for this set of experiments. Future directions include looking at viable antibodies for these proteins, as well as other cell surface receptors to further analyze the immuno-characteristics of these cardiac resident Sca-1^+ and c-kit^+ cells.

4.4 Conclusions

Our study demonstrates that cardiac resident Sca-1^+ cells are EPC-like cells from the heart, which may contribute to vascular adaptation during heart diseases. Importantly, these cells were highly abundant in the RV and reduction in these cells was observed during RV remodeling. No sex differences were observed in the abundance of these cells in healthy rat hearts. These cells may have relevance to vascular adaptation during RV remodeling; however, further studies are needed to define their role in RV vascular adaptation.

REFERENCES

1. Itskovitz-Eldor, J., Schuldiner, M., Karsenti, D., Eden, A., Yanuka, O., Amit, M., ... & Benvenisty, N. (2000). Differentiation of human embryonic stem cells into embryoid bodies compromising the three embryonic germ layers. *Molecular medicine (Cambridge, Mass.),* 6(2), 88-95.

2. Gurusamy, N., Alsayari, A., Rajasingh, S., & Rajasingh, J. (2018). Adult Stem Cells for Regenerative Therapy. *Progress in molecular biology and translational science,* 160, 1-22.

3. Weissman, I.L. (2000). Translating stem and progenitor cell biology to the clinic: barriers and opportunities. *Science (New York, N.Y.),* 287(5457), 1442-6.

4. McCulloch, E.A., & Till, J.E. (2005). Perspectives on the properties of stem cells. *Nature medicine,* 11(10), 1026-8.

5. Steensma, D.P., & Kyle, R. A. (2021). James Till and Ernest McCulloch: Hematopoietic Stem Cell Discoverers. *Mayo Clinic proceedings, 96*(3), 830-831.

6. Simnovitch, L., McCulloch, E.A., & Till, J.E. (1963). The Distribution of Colony-Forming Cells Among Spleen Colonies. *Journal of cellular and comparative physiology,* 62, 327-36.

7. Sobhani, A., Khanlarkhani, N., Baazm, M., Mohammadzadeh, F., Najafi, A., Mehdinejadiani, S., & Sargozaei Aval, F. (2017). Multipotent Stem Cell and Current Application. *Acta medica Iranica, 55*(1), 6-23.

8. Takahashi, K., & Yamanaka, s. (2006). Induction of pluripotent stem cells from mouse embryonic and adult fibroblast cultures by defined factors. *Cells, 126*(4), 663-676.

9. Yamanaka, S. (2008). Induction of pluripotent stem cells from mouse fibroblasts by four transcription factors. *Cell proliferation,* 41 Suppl 1, 51-6.

10. Shi, Y., Inoue, H., Wu, J.C., & Yamanaka, S. (2017). Induced pluripotent stem cell technology: a decade of progress. *Nature reviews. Drug discovery,* 16(2), 115-30.

11. Mora, C., Serzanti, M., Consiglio, A., Memo, M., & Dell'Era, P. (2017). Clinical potentials of human pluripotent stem cells. *Cell biology and toxicology,* 33(4), 351-60.

12. Antalis, T.M., Conway, G.D., Peroutka, R.J., & Buzza, M.S. (2016). Membrane-anchored proteases in endothelial cell biology. *Current opinion in hematology,* 23(3), 243-52.

13. Rakocevic, J., Orlic, D., Mitrovic-Ajtic, O., Tomasevic, M., Dobric, M., Zlatic, N., ... & Labudovic-Borovic, M. (2017). Endothelial cell markers from clinician's perspective. *Experimental and molecular pathology,* 102(2), 303-13.

14. Okada, S., Nakauchi, H., Nagayoshi, K., Nishikawa, S., Miura, Y., & Suda, T. (1992). In vivo and in vitro stem cell function of c-kit- and Sca-1-positive murine hematopoietic cells. *Blood,* 80(12), 3044-50.

15. Holmes, C., & Stanford, W.L. (2007). Concise review: stem cell antigen-1: expression, function, and enigma. *Stem cells (Dayton, Ohio),* 25(6), 1339-47.

16. Yutoku, M., Grossberg, A.L., & Pressman, D. (1974). A cell surface antigenic determinant present on mouse plasmacytes and only about half of mouse thymocytes. *Journal of immunology (Baltimore, Md. : 1950),* 112(5), 1774-81.

17. Upadhyay, G. (2019). Emerging Role of Lymphocyte Antigen-6 Family of Genes in Cancer and Immune Cells. *Frontiers in immunology,* 10, 819.

18. Wang, X., Hu, Q., Nakamura, Y., Lee, J., Zhang, G., From, A.H., & Zhang, J. (2006). The role of the sca-1+/CD31- cardiac progenitor cell population in postinfarction left ventricular remodeling. *Stem cells (Dayton, Ohio),* 24(7), 1779-88.

19. Lennartsson, J., & Rönnstrand, L. (2012). Stem cell factor receptor/c-Kit: from basic science to clinical implications. *Physiological reviews,* 92(4), 1619-49.

20. Hemmings, B.A., & Restuccia, D.F. (2012). PI3K-PKB/Akt pathway. *Cold Spring Harbor perspectives in biology,* 4(9), a011189.

21. Parsons, S.J., & Parsons, J.T. (2004). Src family kinases, key regulators of signal transduction. *Oncogene,* 23(48), 7906-9.

22. Zhang, W., & Liu, H.T. (2002). MAPK signal pathways in the regulation of cell proliferation in mammalian cells. *Cell research,* 12(1), 9-18.

23. Heissig, B., Werb, Z., Rafii, S., & Hattori, K. (2003). Role of c-kit/Kit ligand signaling in regulating vasculogenesis. *Thrombosis and haemostasis,* 90(4), 570-6.

24. Pinto, A.R., Ilinykh, A., Ivey, M.J., Kuwabara, J.T., D'Antoni, M.L., Debuque, R., ... & Tallquist, M.D. (2016). Revisiting Cardiac Cellular Composition. *Circulation research,* 118(3), 400-9.

25. Bolli, R., Tang, X.L., Guo, Y., & Li, Q. (2021). After the storm: an objective appraisal of the efficacy of c-kit+ cardiac progenitor cells in preclinical models of heart disease. *Canadian journal of physiology and pharmacology,* 99(2), 129-39.

26. Tang, X.L., Rokosh, G., Sanganalmath, S.K., Yuan, F., Sato, H., Mu, J., ... & Bolli, R. (2010). Intracoronary administration of cardiac progenitor cells alleviates left ventricular dysfunction in rats with a 30-day-old infarction. *Circulation,* 121(2), 293-305.

27. Sultana, N., Zhang, L., Yan, J., Chen, J., Cai, W., Razzaque, S., ... & Cai, C.L. (2015). Resident c-kit(+) cells in the heart are not cardiac stem cells. *Nature communications,* 6, 8701.

28. Zhang, L., Sultana, N., Yan, J., Yang, F., Chen, F., Chepurko, E., ... & Cai, C.L. (2018). Cardiac Sca-1+ Cells Are Not Intrinsic Stem Cells for Myocardial Development, Renewal, and Repair. *Circulation,* 138(25), 2919-30.

29. van Berlo, J.H., Kanisicak, O., Maillet, M., Vagnozzi, R.J., Karch, J., Lin, S.C., ... & Molkentin, J.D. (2014). c-kit+ cells minimally contribute cardiomyocytes to the heart. *Nature,* 509(7500), 337-41.

30. Vagnozzi, R.J., Sargent, M.A., Lin, S.J., Palpant, N.J., Murry, C.E., & Molkentin, J.D. (2018). Genetic Lineage Tracing of Sca-1+ Cells Reveals Endothelial but Not Myogenic Contribution to the Murine Heart. *Circulation,* 138(25), 2931-9.

31. Cong, X., & Kong, W. (2020). Endothelial tight junctions and their regulatory signaling pathways in vascular homeostasis and disease. *Cellular signalling,* 66, 109485.

32. Baluk, P., Morikawa, S., Haskell, A., Mancuso, M., & McDonald, D.M. (2003). Abnormalities of basement membrane on blood vessels and endothelial sprouts in tumors. *The American journal of pathology,* 163(5), 1801-15.

33. Kumar, G., Dey, S.K., & Kundu, S. (2020). Functional implications of vascular endothelium in regulation of endothelial nitric oxide synthesis to control blood pressure and cardiac functions. *Life sciences,* 259, 118377.

34. Broos, K., Feys, H.B., De Meyer, S.F., Vanhoorelbeke, K., & Deckmyn, H. (2011). Platelets at work in primary hemostasis. *Blood reviews,* 25(4), 155-67.

35. Liu, B., Zhou, H., Zhang, T., Gao, X., Tao, B., Xing, H., ... & Goodwin, J.E. (2021). Loss of endothelial glucocorticoid receptor promotes angiogenesis via upregulation of Wnt/β-catenin pathway. *Angiogenesis,* 24(3), 631-45.

36. Faris, B., Mozzicato, P., Mogayzel, P.J., Ferrera, R., Gerstenfeld, L.C., Glembourtt, M., ... & Franzblau, C. (1983). Effect of protein-hydroxyethylmethacrylate hydrogels on cultured endothelial cells. *Experimental cell research,* 143(1), 15-25.

37. Lertkiatmongkol, P., Liao, D., Mei, H., Hu, Y., & Newman, P.J. (2016). Endothelial functions of platelet/endothelial cell adhesion molecule-1 (CD31). *Current opinion in hematology,* 23(3), 253-9.

38. Paddock, C., Zhou, D., Lertkiatmongkol, P., Newman, P.J., & Zhu, J. (2016). Structural basis for PECAM-1 homophilic binding. *Blood,* 127(8), 1052-61.

39. Mead, L.E., Prater, D., Yoder, M.C., & Ingram, D.A. (2008). Isolation and characterization of endothelial progenitor cells from human blood. *Current protocols in stem cell biology,* Chapter 2, Unit 2C.1.

40. Voyta, J.C., Via, D.P., Butterfield, C.E., & Zetter, B.R. (1984). Identification and isolation of endothelial cells based on their increased uptake of acetylated-low density lipoprotein. *The Journal of cell biology,* 99(6), 2034-40.

41. Apostolov, E.O., Shah, S.V., Ray, D., & Basnakian, A.G. (2009). Scavenger receptors of endothelial cells mediate the uptake and cellular proatherogenic effects of carbamylated LDL. *Arteriosclerosis, thrombosis, and vascular biology,* 29(10), 1622-30.

42. Acton, S.L., Scherer, P.E., Lodish, H.F., & Krieger, M. (1994). Expression cloning of SR-BI, a CD36-related class B scavenger receptor. *The Journal of biological chemistry,* 269(33), 21003-9.

43. Park Y. M. (2014). CD36, a scavender receptor implicated in atherosclerosis. *Experimental & molecular medicine, 46*(6), e99.

44. Pritchard, K.A., Groszek, L., Smalley, D.M., Sessa, W.C., Wu, M., Villalon, P., ... & Stemerman, M.B. (1995). Native low-density lipoprotein increases endothelial cell nitric oxide synthase generation of superoxide anion. *Circulation research,* 77(3), 510-8.

45. Laitinen, L. (1987). Griffonia simplicifolia lectins bind specifically to endothelial cells and some epithelial cells in mouse tissues. *The Histochemical journal,* 19(4), 225-34.

46. Aisenbrey, E.A., & Murphy, W.L. (2020). Synthetic alternatives to Matrigel. *Nature reviews. Materials,* 5(7), 539-51.

47. Hughes, C.S., Postovit, L.M., & Lajoie, G.A. (2010). Matrigel: a complex protein mixture required for optimal growth of cell culture. *Proteomics,* 10(9), 1886-90.

48. Baatout, S., & Cheţa, N. (1996). Matrigel: a useful tool to study endothelial differentiation. *Romanian journal of internal medicine = Revue roumaine de medecine interne,* 34(3-4), 263-9.

49. Kozlowski, M.T., Crook, C.J., & Ku, H.T. (2021). Towards organoid culture without Matrigel. *Communications biology,* 4(1), 1387.

50. Davidson, C.D., Wang, W.Y., Zaimi, I., Jayco, D.K.P., & Baker, B.M. (2019). Cell force-mediated matrix reorganization underlies multicellular network assembly. *Scientific reports,* 9(1), 12.

51. Asahara, T., Murohara, T., Sullivan, A., Silver, M., van der Zee, R., Li, T., ... & Isner, J.M. (1997). Isolation of putative progenitor endothelial cells for angiogenesis. *Science (New York, N.Y.),* 275(5302), 964-7.

52. Walter, D.H., Rittig, K., Bahlmann, F.H., Kirchmair, R., Silver, M., Murayama, T., ... & Isner, J.M. (2002). Statin therapy accelerates reendothelialization: a novel effect involving mobilization and incorporation of bone marrow-derived endothelial progenitor cells. *Circulation,* 105(25), 3017-24.

53. Keighron, C., Lyons, C.J., Creane, M., O'Brien, T., & Liew, A. (2018). Recent Advances in Endothelial Progenitor Cells Toward Their Use in Clinical Translation. *Frontiers in medicine,* 5, 354.

54. Cristóvão, G., Milner, J., Sousa, P., Ventura, M., Cristóvão, J., Elvas, L., ... & António, N. (2020). Improvement in circulating endothelial progenitor cells pool after cardiac resynchronization therapy: increasing the list of benefits. *Stem cell research & therapy,* 11(1), 194.

55. Hill, J.M., Zalos, G., Halcox, J.P., Schenke, W.H., Waclawiw, M.A., Quyyumi, A.A., & Finkel, T. (2003). Circulating endothelial progenitor cells, vascular function, and cardiovascular risk. *The New England journal of medicine,* 348(7), 593-600.

56. Murasawa, S., & Asahara, T. (2005). Endothelial progenitor cells for vasculogenesis. *Physiology (Bethesda, Md.),* 20, 36-42.

57. Werner, N., Kosiol, S., Schiegl, T., Ahlers, P., Walenta, K., Link, A., ... & Nickenig, G. (2005). Circulating endothelial progenitor cells and cardiovascular outcomes. *The New England journal of medicine,* 353(10), 999-1007.

58. Lara-Hernandez, R., Lozano-Vilardell, P., Blanes, P., Torreguitart-Mirada, N., Galmés, A., & Besalduch, J. (2010). Safety and efficacy of therapeutic angiogenesis as a novel treatment in patients with critical limb ischemia. *Annals of vascular surgery,* 24(2), 287-94.

59. Obtake, T., Mochida, Y., Ishioka, K., Oka, M., Maesato, K., Moriya, H., … & Kobayashi, S. (2018). Autologous Granulocyte Colony-Stimulating Factor-Mobilized Peripheral Blood CD34 Positive Cell Transplantation for Hemodialysis Patients with Critical Limb Ischemia: A Prospective Phase II Clinical Trial. *Stem cells translational medicine,* 7(11), 774-82.

60. Zhu, J., Song, J., Yu, L., Zheng, H., Zhou, B., Weng, S., & Fu, G. (2016). Safety and efficacy of autologous thymosin β4 pre-treated endothelial progenitor cell transplantation in patients with acute ST segment elevation myocardial infarction: A pilot study. *Cytotherapy,* 18(8), 1037-42.

61. Granton, J., Langleben, D., Kutryk, M.B., Camack, N., Galipeau, J., Courtman, D.W., & Stewart, D.J. (2015). Endothelial NO-Synthase Gene-Enhanced Progenitor Cell Therapy for Pulmonary Arterial Hypertension: The PHACeT Trial. *Circulation research,* 117(7), 645-54.

62. Yoder, M.C. (2012). Human endothelial progenitor cells. *Cold Spring Harbor perspectives in medicine,* 2(7), a006692.

63. Bartlett, A.L., Grewal, T., De Angelis, E., Myers, S., & Stanley, K.K. (2000). Role of the macrophage galactose lectin in the uptake of desialylated LDL. *Atherosclerosis,* 153(1), 219-30.

64. Ryter, A. (1985). Relationship between ultrastructure and specific functions of macrophages. *Comparative immunology, microbiology and infectious diseases,* 8(2), 119-33.

65. Case, J., Mead, L.E., Bessler, W.K., Prater, D., White, H.A., Saadatzadeh, M.R., ... & Ingram, D.A. (2007). Human CD34+AC133+VEGFR-2+ cells are not endothelial progenitor cells but distinct, primitive hematopoietic progenitors. *Experimental hematology,* 35(7), 1109-18.

66. Hur, J., Yoon, C.H., Kim, H.S., Choi, J.H., Kang, H.J., Hwang, K.K., ... & Park, Y.B. (2004). Characterization of two types of endothelial progenitor cells and their different contributions to neovasculogenesis. *Arteriosclerosis, thrombosis, and vascular biology,* 24(2), 288-93.

67. Yoder, M.C., Mead, L.E., Prater, D., Krier, T.R., Mroueh, K.N., Li, F., ... & Ingram, D.A. (2007). Redefining endothelial progenitor cells via clonal analysis and hematopoietic stem/progenitor cell principals. *Blood,* 109(5), 1801-9.

68. Medina, R.J., Barber, C.L., Sabatier, F., Dignat-George, F., Melero-Martin, J.M., Khosrotehrani, K., ... & Stitt, A.W. (2017). Endothelial Progenitors: A Consensus Statement on Nomenclature. *Stem cells translational medicine,* 6(5), 1316-20.

69. Ray, R., Novotny, N.M., Crisostomo, P.R., Lahm, T., Abarbanell, A., & Meldrum, D.R. (2008). Sex steroids and stem cell function. *Molecular medicine (Cambridge, Mass.),* 14(7-8), 493-501.

70. Hermann, J.L., Abarbanell, A.M., Weil, B.R., Manukyan, M.C., Poynter, J.A., Wang, Y., … & Meldrum, D.R. (2010). Gender dimorphisms in progenitor and stem cell function in cardiovascular disease. *Journal of cardiovascular translational research,* 3(2), 103-13.

71. Zhen, Y., Xiao, S., Ren, Z., Shen, H.W., Su, H., Tang, Y.B., & Zeng, H. (2015). Increased endothelial progenitor cells and nitric oxide in young prehypertensive women. *Journal of clinical hypertension (Greenwich, Conn.),* 17(4), 298-305.

72. Itzhaki-Alfia, A., Leor, J., Raanani, E., Sternik, L., Spiegelstein, D., Netser, S., ... & Barbash, I.M. (2009). Patient characteristics and cell source determine the number of isolated human cardiac progenitor cells. *Circulation,* 120(25), 2559-66.

73. Lemieux, C., Cloutier, I., & Tanguay, J.F. (2009). Menstrual cycle influences endothelial progenitor cell regulation: a link to gender differences in vascular protection. *International journal of cardiology,* 136(2), 200-10.

74. Tanaka, S., Ueno, T., Sato, F., Chigusa, Y., Kawaguchi-Sakita, N., Kawashima, M., ... & Toi, M. (2012). Alterations of circulating endothelial cell and endothelial progenitor cell counts around the ovulation. *The Journal of clinical endocrinology and metabolism,* 97(11), 4182-92.

75. Imanishi, T., Tsujioka, H., & Akasaka, T. (2010). Endothelial progenitor cell senescence--is there a role for estrogen. *Therapeutic advances in cardiovascular disease,* 4(1), 55-69.

76. Matsubara, Y., & Matsubara, K. (2012). Estrogen and progesterone play pivotal roles in endothelial progenitor cell proliferation. *Reproductive biology and endocrinology : RB&E,* 10, 2.

77. Wang, L., Gu, H., Turrentine, M., & Wang, M. (2014). Estradiol treatment promotes cardiac stem cell (CSC)-derived growth factors, thus improving CSC-mediated cardioprotection after acute ischemia/reperfusion. *Surgery,* 156(2), 243-52.

78. Iwakura, A., Shastry, S., Luedemann, C., Hamada, H., Kawamoto, A., Kishore, R., ... & Losordo, D.W. (2006). Estradiol enhances recovery after myocardial infarction by augmenting incorporation of bone marrow-derived endothelial progenitor cells into sites of ischemia-induced neovascularization via endothelial nitric oxide synthase-mediated activation of matrix metalloproteinase-9. *Circulation,* 113(12), 1605-14.

79. Baruscotti, I., Barchiesi, F., Jackson, E.K., Imthurn, B., Stiller, R., Kim, J.H., ... & Dubey, R.K. (2010). Estradiol stimulates capillary formation by human endothelial progenitor cells: role of estrogen receptor-{alpha}/{beta}, heme oxygenase 1, and tyrosine kinase. *Hypertension (Dallas, Tex. : 1979),* 56(3), 397-404.

80. Yu, P., Zhang, Z., Li, S., Wen, X., Quan, W., Tian, Q., ... & Jiang, R. (2016). Progesterone modulates endothelial progenitor cell (EPC) viability through the CXCL12/CXCR4/PI3K/Akt signalling pathway. *Cell proliferation,* 49(1), 48-57.

81. van der Bruggen, C.E.E., Tedford, R.J., Handoko, M.L., van der Velden, J., & de Man, F.S. (2017). RV pressure overload: from hypertrophy to failure. *Cardiovascular research,* 113(12), 1423-32.

82. Burke, M.A., Katz, D.H., Beussink, L., Selvaraj, S., Gupta, D.K., Fox, J., ... & Shah, S.J. (2014). Prognostic importance of pathophysiologic markers in patients with heart failure and preserved ejection fraction. *Circulation. Heart failure,* 7(2), 288-99.

83. Mohammed, S.F., Hussain, I., AbouEzzeddine, O.F., Abou Ezzeddine, O.F., Takahama, H., Kwon, S.H., ... & Redfield, M.M. (2014). Right ventricular function in heart failure with preserved ejection fraction: a community-based study. *Circulation,* 130(25), 2310-20.

84. Iglesias-Garriz, I., Olalla-Gómez, C., Garrote, C., López-Benito, M., Martín, J., Alonso, D., & Rodríguez, M.A. (2012). Contribution of right ventricular dysfunction to heart failure mortality: a meta-analysis. *Reviews in cardiovascular medicine,* 13(2-3), e62-9.

85. Konstam, M.A., Kiernan, M.S., Bernstein, D., Bozkurt, B., Jacob, M., Kapur, N.K., ... & Ward, C. (2018). Evaluation and Management of Right-Sided Heart Failure: A Scientific Statement From the American Heart Association. *Circulation,* 137(20), e578-e622.

86. Puwanant, S., Priester, T.C., Mookadam, F., Bruce, C.J., Redfield, M.M., & Chandrasekaran, K. (2009). Right ventricular function in patients with preserved and reduced ejection fraction heart failure. *European journal of echocardiography : the journal of the Working Group on Echocardiography of the European Society of Cardiology,* 10(6), 733-7.

87. Frea, S., Pidello, S., Bovolo, V., Iacovino, C., Franco, E., Pinneri, F., ... & Gaita, F. (2016). Prognostic incremental role of right ventricular function in acute decompensation of advanced chronic heart failure. *European journal of heart failure,* 18(5), 564-72.

88. van de Veerdonk, M.C., Kind, T., Marcus, J.T., Mauritz, G.J., Heymans, M.W., Bogaard, H.J., ... & Vonk-Noordegraaf, A. (2011). Progressive right ventricular dysfunction in patients with pulmonary arterial hypertension responding to therapy. *Journal of the American College of Cardiology,* 58(24), 2511-9.

89. Zelt, J.G.E., Chaudhary, K.R., Cadete, V.J., Mielniczuk, L.M., & Stewart, D.J. (2019). Medical Therapy for Heart Failure Associated With Pulmonary Hypertension. *Circulation research,* 124(11), 1551-67.

90. Andersen, S., Schultz, J.G., Andersen, A., Ringgaard, S., Nielsen, J.M., Holmboe, S., ... & Nielsen-Kudsk, J.E. (2014). Effects of bisoprolol and losartan treatment in the hypertrophic and failing right heart. *Journal of cardiac failure,* 20(11), 864-73.

91. Borgdorff, M.A., Bartelds, B., Dickinson, M.G., Steendijk, P., & Berger, R.M. (2013). A cornerstone of heart failure treatment is not effective in experimental right ventricular failure. *International journal of cardiology,* 169(3), 183-9.

92. Reddy, S., & Bernstein, D. (2015). The vulnerable right ventricle. *Current opinion in pediatrics,* 27(5), 563-8.

93. Kasahara, Y., Kiyatake, K., Tatsumi, K., Sugito, K., Kakusaka, I., Yamagata, S., ... & Kuriyama, T. (1997). Bioactivation of monocrotaline by P-450 3A in rat liver. *Journal of cardiovascular pharmacology,* 30(1), 124-9.

94. Xiao, R., Su, Y., Feng, T., Sun, M., Liu, B., Zhang, J., ... & Hu, Q. (2017). Monocrotaline Induces Endothelial Injury and Pulmonary Hypertension by Targeting the Extracellular Calcium-Sensing Receptor. *Journal of the American Heart Association,* 6(4), e004865.

95. Suparmi, S., Wesseling, S., & Rietjens, I.M.C.M. (2020). Monocrotaline-induced liver toxicity in rat predicted by a combined in vitro physiologically based kinetic modeling approach. *Archives of toxicology,* 94(9), 3281-95.

96. Gomez-Arroyo, J.G., Farkas, L., Alhussaini, A.A., Farkas, D., Kraskauskas, D., Voelkel, N.F., & Bogaard, H.J. (2012). The monocrotaline model of pulmonary hypertension in perspective. *American journal of physiology. Lung cellular and molecular physiology,* 302(4), L363-9.

97. Al-Husseini, A., Kraskauskas, D., Mezzaroma, E., Nordio, A., Farkas, D., Drake, J.I., ... & Voelkel, N.F. (2015). Vascular endothelial growth factor receptor 3 signaling contributes to angioobliterative pulmonary hypertension. *Pulmonary circulation,* 5(1), 101-16.

98. Jiang, B., Deng, Y., Suen, C., Taha, M., Chaudhary, K.R., Courtman, D.W., & Stewart, D.J. (2016). Marked Strain-Specific Differences in the SU5416 Rat Model of Severe Pulmonary Arterial Hypertension. *American journal of respiratory cell and molecular biology,* 54(4), 461-8.

99. Bogaard, H.J., Legchenko, E., Ackermann, M., Kühnel, M.P., Jonigk, D.D., Chaudhary, K.R., ... & Hansmann, G. (2020). The Adult Sprague-Dawley Sugen-Hypoxia Rat Is Still "the One:" A Model of Group 1 Pulmonary Hypertension: Reply to Le Cras and Abman. *American journal of respiratory and critical care medicine,* 201(5), 621-4.

100. Hirata, M., Ousaka, D., Arai, S., Okuyama, M., Tarui, S., Kobayashi, J., ... & Sano, S. (2015). Novel Model of Pulmonary Artery Banding Leading to Right Heart Failure in Rats. *BioMed research international,* 2015, 753210.

101. Akazawa, Y., Okumura, K., Ishii, R., Slorach, C., Hui, W., Ide, H., ... & Friedberg, M.K. (2020). Pulmonary artery banding is a relevant model to study the right ventricular remodeling and dysfunction that occurs in pulmonary arterial hypertension. *Journal of applied physiology (Bethesda, Md. : 1985),* 129(2), 238-46.

102. Brower, M., Grace, M., Kotz, C.M., & Koya, V. (2015). Comparative analysis of growth characteristics of Sprague Dawley rats obtained from different sources. *Laboratory animal research,* 31(4), 166-73.

103. Suen, C.M., Chaudhary, K.R., Deng, Y., Jiang, B., & Stewart, D.J. (2019). Fischer rats exhibit maladaptive structural and molecular right ventricular remodelling in severe pulmonary hypertension: a genetically prone model for right heart failure. *Cardiovascular research,* 115(4), 788-99.

104. Kolb, T.M., Peabody, J., Baddoura, P., Fallica, J., Mock, J.R., Singer, B.D., ... & Hassoun, P.M. (2015). Right Ventricular Angiogenesis is an Early Adaptive Response to Chronic Hypoxia-Induced Pulmonary Hypertension. *Microcirculation (New York, N.Y. : 1994),* 22(8), 724-36.

105. Potus, F., Ruffenach, G., Dahou, A., Thebault, C., Breuils-Bonnet, S., Tremblay, È., ... & Bonnet, S. (2015). Downregulation of MicroRNA-126 Contributes to the Failing Right Ventricle in Pulmonary Arterial Hypertension. *Circulation,* 132(10), 932-43.

106. Patel, R.B., Li, E., Benefield, B.C., Swat, S.A., Polsinelli, V.B., Carr, J.C., ... & Freed, B.H. (2020). Diffuse right ventricular fibrosis in heart failure with preserved ejection fraction and pulmonary hypertension. *ESC heart failure,* 7(1), 253-63.

107. Andersen, S., Birkmose Axelsen, J., Ringgaard, S., Randel Nyengaard, J., Holm Nielsen, S., Genovese, F., ... & Andersen, A. (2019). Pressure overload induced right ventricular remodeling is not attenuated by the anti-fibrotic agent pirfenidone. *Pulmonary circulation,* 9(2), 2045894019848659.

108. Hagdorn, Q.A.J., Kurakula, K., Koop, A.C., Bossers, G.P.L., Mavrogiannis, E., van Leusden, T., ... & Berger, R.M.F. (2021). Volume Load-Induced Right Ventricular Failure in Rats Is Not Associated With Myocardial Fibrosis. *Frontiers in physiology,* 12, 557514.

109. Rich, S., Pogoriler, J., Husain, A.N., Toth, P.T., Gomberg-Maitland, M., & Archer, S.L. (2010). Long-term effects of epoprostenol on the pulmonary vasculature in idiopathic pulmonary arterial hypertension. *Chest,* 138(5), 1234-9.

110. Piao, L., Fang, Y.H., Cadete, V.J., Wietholt, C., Urboniene, D., Toth, P.T., ... & Archer, S.L. (2010). The inhibition of pyruvate dehydrogenase kinase improves impaired cardiac function and electrical remodeling in two models of right ventricular hypertrophy: resuscitating the hibernating right ventricle. *Journal of molecular medicine (Berlin, Germany),* 88(1), 47-60.

111. Voelkel, N.F., Bogaard, H.J., Al Husseini, A., Farkas, L., Gomez-Arroyo, J., & Natarajan, R. (2013). Antioxidants for the treatment of patients with severe angioproliferative pulmonary hypertension. *Antioxidants & redox signaling,* 18(14), 1810-7.

112. Dolenc, J., Šebeštjen, M., Vrtovec, B., Koželj, M., & Haddad, F. (2014). Pulmonary hypertension in patients with advanced heart failure is associated with increased levels of interleukin-6. *Biomarkers : biochemical indicators of exposure, response, and susceptibility to chemicals,* 19(5), 385-90.

113. Campian, M.E., Hardziyenka, M., de Bruin, K., van Eck-Smit, B.L., de Bakker, J.M., Verberne, H.J., & Tan, H.L. (2010). Early inflammatory response during the development of right ventricular heart failure in a rat model. *European journal of heart failure,* 12(7), 653-8.

114. Rondelet, B., Dewachter, C., Kerbaul, F., Kang, X., Fesler, P., Brimioulle, S., ... & Dewachter, L. (2012). Prolonged overcirculation-induced pulmonary arterial hypertension as a cause of right ventricular failure. *European heart journal,* 33(8), 1017-26.

115. Hemnes, A.R., Maynard, K.B., Champion, H.C., Gleaves, L., Penner, N., West, J., & Newman, J.H. (2012). Testosterone negatively regulates right ventricular load stress responses in mice. *Pulmonary circulation,* 2(3), 352-8.

116. Wang, Y.D., Li, Y.D., Ding, X.Y., Wu, X.P., Li, C., Guo, D.C., ... & Lu, X.Z. (2019). 17β-estradiol preserves right ventricular function in rats with pulmonary arterial hypertension: an echocardiographic and histochemical study. *The international journal of cardiovascular imaging,* 35(3), 441-50.

117. Liu, A., Philip, J., Vinnakota, K.C., Van den Bergh, F., Tabima, D.M., Hacker, T., ... & Chesler, N.C. (2017). Estrogen maintains mitochondrial content and function in the right ventricle of rats with pulmonary hypertension. *Physiological reports,* 5(6), e13157.

118. Guihaire, J., Deuse, T., Wang, D., Fadel, E., Reichenspurner, H., & Schrepfer, S. (2015). Sex Differences in Immunology: More Severe Development of Experimental Pulmonary Hypertension in Male Rats Exposed to Vascular Endothelial Growth Factor Receptor Blockade. *BioMed research international,* 2015, 765292.

119. Hangartner, J.R., Marley, N.J., Whitehead, A., Thomas, A.C., & Davies, M.J. (1985). The assessment of cardiac hypertrophy at autopsy. *Histopathology,* 9(12), 1295-306.

120. Chen, C., Dai, P., Nan, L., Lu, R., Wang, X., Tian, Y., ... & Zhang, Y. (2021). Isolation and characterization of endothelial progenitor cells from canine bone marrow. *Biotechnic & histochemistry : official publication of the Biological Stain Commission,* 96(2), 85-93.

121. Berglund, F., Piña, P., & Herrera, C.J. (2020). Right ventricle in heart failure with preserved ejection fraction. *Heart (British Cardiac Society),* 106(23), 1798-804.

122. de Man, F.S., & Naeije, R. (2021). Sex and the Right Ventricle in Heart Failure With Preserved Ejection Fraction. *Chest,* 159(6), 2156-8.

123. Sisakian, S.A., & Matevosian, R.S. (1982). Capillary system of rat myocardium in experimental hypertrophy and physical exercise. *Cor et vasa,* 24(5), 381-8.

124. Bogaard, H.J., Natarajan, R., Henderson, S.C., Long, C.S., Kraskauskas, D., Smithson, L., ... & Voelkel, N.F. (2009). Chronic pulmonary artery pressure elevation is insufficient to explain right heart failure. *Circulation,* 120(20), 1951-60.

125. Nogueira-Ferreira, R., Vitorino, R., Ferreira, R., & Henriques-Coelho, T. (2015). Exploring the monocrotaline animal model for the study of pulmonary arterial hypertension: A network approach. *Pulmonary pharmacology & therapeutics,* 35, 8-16.

126. Thomas, H.C., Lamé, M.W., Dunston, S.K., Segall, H.J., & Wilson, D.W. (1998). Monocrotaline pyrrole induces apoptosis in pulmonary artery endothelial cells. *Toxicology and applied pharmacology,* 151(2), 236-44.

127. Aref, Z., & Ouax, P.H.A. (2021). In Vivo Matrigel Plug Assay as a Potent Method to Investigate Specific Individual Contribution of Angiogenesis to Blood Flow Recovery in Mice. *International journal of molecular sciences,* 22(16), 8909.